Cell Reports

Article

Airway extracellular LTA_4H concentrations are governed by release from liver hepatocytes and changes in lung vascular permeability

Graphical abstract

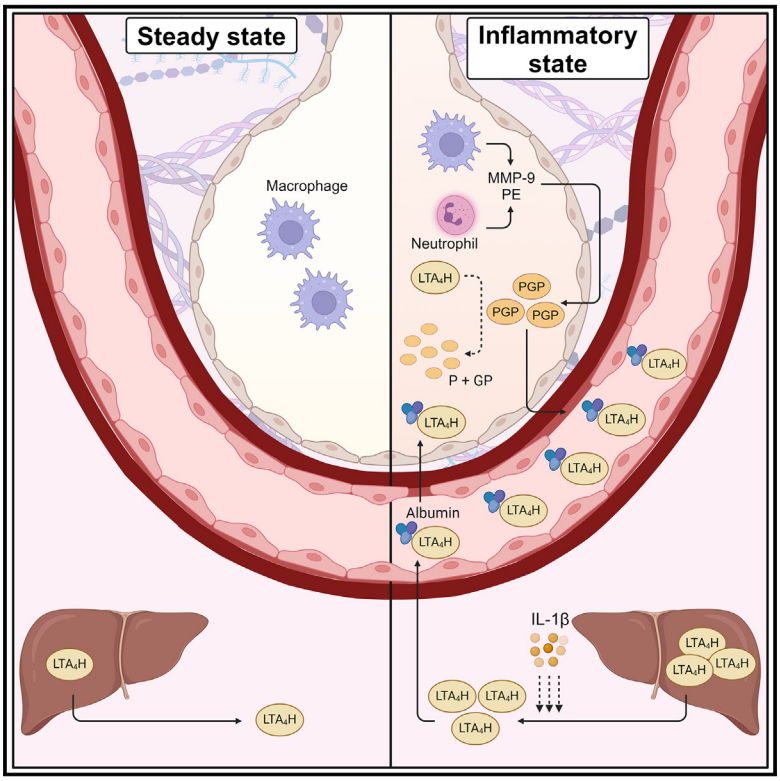

Authors

Kyle T. Mincham, Samia Akthar, Dhiren F. Patel, ..., Amit Gaggar, James E. Blalock, Robert J. Snelgrove

Correspondence

robert.snelgrove@imperial.ac.uk

In brief

Mincham et al. define pathways governing the bioavailability of extracellular leukotriene A_4 hydrolase (LTA_4H). LTA_4H's location defines its function, whereby it generates leukotriene B_4 intracellularly but degrades proline-glycine-proline extracellularly. Airway extracellular LTA_4H concentrations are governed by changes in vascular permeability and influx of blood-borne enzyme, which is in turn secreted by liver hepatocytes.

Highlights

- LTA_4H operates intracellularly to generate LTB_4 and extracellularly to degrade PGP
- The previously unknown origin of extracellular LTA_4H was shown to be liver hepatocytes
- Constitutive LTA_4H release into blood is enhanced during an acute phase response
- Extracellular airway LTA_4H levels are dictated by changes in vascular permeability

Mincham et al., 2024, Cell Reports *43*, 114630
August 27, 2024
https://doi.org/10.1016/j.celrep.2024.114630

CellPress

Cell Reports

CellPress
OPEN ACCESS

Article

Airway extracellular LTA_4H concentrations are governed by release from liver hepatocytes and changes in lung vascular permeability

Kyle T. Mincham,[1] Samia Akthar,[1] Dhiren F. Patel,[1,2] Garance F. Meyer,[1] Clare M. Lloyd,[1] Amit Gaggar,[3,4,5,6] James E. Blalock,[3,4,5] and Robert J. Snelgrove[1,7,*]

[1]Inflammation Repair and Development, National Heart and Lung Institute, Imperial College London, London SW7 2AZ, UK
[2]Department of Cellular Microbiology, Max Planck Institute for Infection Biology, Charitéplatz 1, 10117 Berlin, Germany
[3]Division of Pulmonary, Allergy & Critical Care Medicine, Department of Medicine, University of Alabama at Birmingham, Birmingham, AL, USA
[4]Program in Protease and Matrix Biology, University of Alabama at Birmingham, Birmingham, AL, USA
[5]Lung Health Center and Gregory Fleming James CF Center, University of Alabama at Birmingham, Birmingham, AL, USA
[6]Birmingham VA Medical Center, Birmingham, AL, USA
[7]Lead contact
*Correspondence: robert.snelgrove@imperial.ac.uk
https://doi.org/10.1016/j.celrep.2024.114630

SUMMARY

Leukotriene A_4 hydrolase (LTA_4H) is a bifunctional enzyme, with dual activities critical in defining the scale of tissue inflammation and pathology. LTA_4H classically operates intracellularly, primarily within myeloid cells, to generate pro-inflammatory leukotriene B_4. However, LTA_4H also operates extracellularly to degrade the bioactive collagen fragment proline-glycine-proline to limit neutrophilic inflammation and pathological tissue remodeling. While the dichotomous functions of LTA_4H are dictated by location, the cellular source of extracellular enzyme remains unknown. We demonstrate that airway extracellular LTA_4H concentrations are governed by the level of pulmonary vascular permeability and influx of an abundant repository of blood-borne enzyme. In turn, blood LTA_4H originates from liver hepatocytes, being released constitutively but further upregulated during an acute phase response. These findings have implications for our understanding of how inflammation and repair are regulated and how perturbations to the LTA_4H axis may manifest in pathologies of chronic diseases.

INTRODUCTION

In response to lung infection or injury, it is critical that the host elicits inflammatory and reparative processes to combat threats from invading pathogens and restore tissue integrity and function. However, it is also critical that these processes are tightly regulated since their dysregulation can result in persistent, non-resolving inflammation and pathological structural changes termed tissue remodeling. These are hallmark features of many chronic lung diseases (CLDs), and thus, a greater understanding of processes that regulate inflammation and repair are of the utmost importance.

The enzyme leukotriene A_4 hydrolase (LTA_4H) classically operates as an epoxide hydrolase, whereby it functions intracellularly, primarily within myeloid cells, to convert leukotriene A_4 (LTA_4) into pro-inflammatory lipid mediator leukotriene B_4 (LTB_4).[1–6] LTB_4 is a potent chemotactic factor and activator for various inflammatory cells, implicated both in host defense but also pathological inflammation and tissue remodeling when its production is dysregulated.[6–10] However, LTA_4H is a bifunctional enzyme, whereby it also operates in an extracellular environment to degrade the bioactive collagen fragment tripeptide proline-glycine-proline (PGP).[11] In response to infection or injury, PGP is liberated from collagen of the extracellular matrix through the sequential enzymatic activities of matrix metalloproteinases (MMP-8 and MMP-9) and prolyl endopeptidase (PE).[10–13] PGP classically functions as a neutrophil chemoattractant and activator.[14] More recently, a pro-reparative role for PGP has also been suggested, whereby it drives the proliferation, chemotaxis and tube-forming capacity of endothelial progenitor cells and the proliferation and spreading of airway epithelial cell progenitors.[12,15,16] Thus, it has been rationalized that PGP is liberated during injury and then operates to guide a proximal repair and sterilization response.[12] In this setting, PGP bioavailability is defined by the activity of extracellular LTA_4H, and during an acute self-resolving inflammatory response, both PGP generation and degradation are coordinated to ensure that PGP is unable to persist.[10–12] A failure of extracellular LTA_4H to efficiently degrade PGP results in a greater and more prolonged neutrophilic inflammation and pathological epithelial remodeling.[10,16] Accordingly, extracellular LTA_4H levels and/or activity are reduced in numerous CLDs resulting in PGP accumulation and associated pathology.[16–19]

LTA_4H is therefore an unusual, bifunctional enzyme, the action of which is defined by its cellular location: intracellularly it promotes inflammation through LTB_4 generation, whereas extracellularly, it limits inflammation and pathological remodeling by degrading PGP.[12,20] The balance of these dual activities is thus critical in defining the magnitude and duration of inflammatory and reparative responses and dictating the distinction between protective versus pathological outcomes. However, the cellular source of extracellular LTA_4H and the mechanisms that govern its release remain unknown. In episodes of acute, self-resolving pulmonary inflammation, elevations in extracellular LTA_4H temporally align with infiltration of neutrophils into the airways.[10,11] Since neutrophils are a rich source of intracellular LTA_4H, it had been postulated that they may also represent a primary source of extracellular enzyme. In this study, we demonstrate that airway extracellular LTA_4H surprisingly originates from the blood, and that its levels in bronchoalveolar lavage fluid (BALF) are defined by the extent of vascular permeability. Neutrophilic airway infiltration promotes vascular permeability and thus indirectly promotes elevations in extracellular LTA_4H, which in turn operates to degrade PGP and limit neutrophilia. Conversely, vasoactive agents directly promote vascular permeability and elevations in extracellular LTA_4H independent of neutrophilic inflammation. We demonstrate that the blood is an abundant source of functional extracellular LTA_4H, which does not seemingly originate from blood-borne cells. Instead, we demonstrate that liver hepatocytes express high levels of LTA_4H, which they release constitutively at steady state, but with release further upregulated as part of an acute phase response. Thus, systemic changes in extracellular LTA_4H and more localized changes in vascular permeability define its extracellular levels in the lung and ultimately govern regulation of local inflammation and repair processes.

RESULTS

Extracellular airway concentrations of LTA_4H correlate with concentrations of albumin

Previous studies have demonstrated that LTA_4H is the only enzyme present in the BALF of mice capable of degrading PGP.[10,11,16] In mouse models of acute, self-resolving, airway inflammation, it has been demonstrated that early increases in BALF LTA_4H concentrations correlated with neutrophilic infiltrate,[10,11] thus suggesting neutrophils were a potential source of the extracellular enzyme. To further interrogate the relationship between airway neutrophilic inflammation and changes in extracellular LTA_4H, mice were administered a range of agonists to distinct Toll-like receptors (TLR), and acute airway changes were assessed after 24 h (Figure 1A). Mice administered distinct TLR agonists displayed a spectrum of total cellular (Figure 1B) and neutrophilic (Figure 1C) responses in their airways, coupled with variable elevations in BALF concentrations of LTA_4H (Figure 1D). While a significant correlation was observed between airway neutrophilic responses and BALF LTA_4H concentrations (Figure 1E) and increased neutrophil numbers universally resulted in a concomitant increase in extracellular LTA_4H (Figures 1C–1E), it was also apparent that augmented BALF LTA_4H levels could be observed in the absence of a pronounced neutrophilia (Figures 1C–1E). Extracellular LTA_4H levels were seemingly not a consequence of cell death as no correlation was observed with levels of BALF lactate dehydrogenase (LDH) (Figure 1F). However, the strongest correlation observed was between BALF concentrations of LTA_4H and albumin (Figure 1G).

To further interrogate these associations temporally, mice were administered LPS, and airway changes were assessed longitudinally (Figure 1H). LPS administration resulted in a significant increase in airway neutrophil numbers (Figure 1I) and BALF LTA_4H concentrations (Figure 1J). However, airway albumin concentrations displayed a comparable increase post LPS administrations (Figure 1K) and demonstrated a significant correlation with BALF LTA_4H levels (Figure 1L). Albumin is a serum protein, with airway concentrations reflective of the level of pulmonary vascular permeability. This raised the possibility that extracellular LTA_4H in the airways was predominantly derived from the blood and that pulmonary levels reflected the extent of vascular permeability.

Serum is an abundant source of extracellular LTA_4H with robust PGP-degrading activity

Concentrations of LTA_4H were subsequently assessed in serum of naive mice and found to be strikingly enriched relative to BALF concentrations of the enzyme (Figure 2A). Accordingly, mouse serum possessed a robust capacity to degrade PGP, as determined by measuring the loss of peptide via mass spectrometry (Figure 2B) and liberation of the N-terminal proline residues (Figure 2C). This PGP-degrading activity was significant even when serum was diluted 100-fold (Figures 2B and 2C), being substantially greater than that observed for naive mouse BAL fluid.[10,11] Importantly, the PGP-degrading activity of serum was abolished in *Lta4h*$^{-/-}$ mice, demonstrating that this is the only serum enzyme capable of degrading PGP (Figures 2D and 2E). LTA_4H is a tripeptide aminopeptidase, and serum PGP-degrading activity was also abolished by incubation with specific tripeptide aminopeptidase inhibitor bestatin (Figure 2F). Serum derived from healthy human volunteers displayed a comparably robust capacity to degrade PGP (Figures 2G and 2H), with activity again abrogated by bestatin (Figure 2I).

Airway extracellular LTA_4H concentrations are defined by the level of vascular permeability

Given the substantial concentrations of LTA_4H in serum and the correlation between airway LTA_4H and albumin concentrations, the role of vascular permeability in defining extracellular BALF LTA_4H concentrations was investigated. During inflammation, a variety of signals can augment vascular permeability through inducing contraction of endothelial cells and loss of adherens/tight junctions.[21] Neutrophil transendothelial migration induces changes in endothelial cells leading to enhanced vascular permeability.[22] Accordingly, administration of neutrophil chemokine MIP-2 to mice (Figure 3A) resulted in robust airway neutrophilic inflammation (Figure 3B), which coincided with increased BALF concentrations of albumin (Figure 3C) and LTA_4H (Figure 3D) and greater BALF PGP-degrading activity (Figures 3E and 3F). BALF LTA_4H concentrations (Figure 3G) and PGP-degrading activity (Figure 3H) significantly correlated with BALF

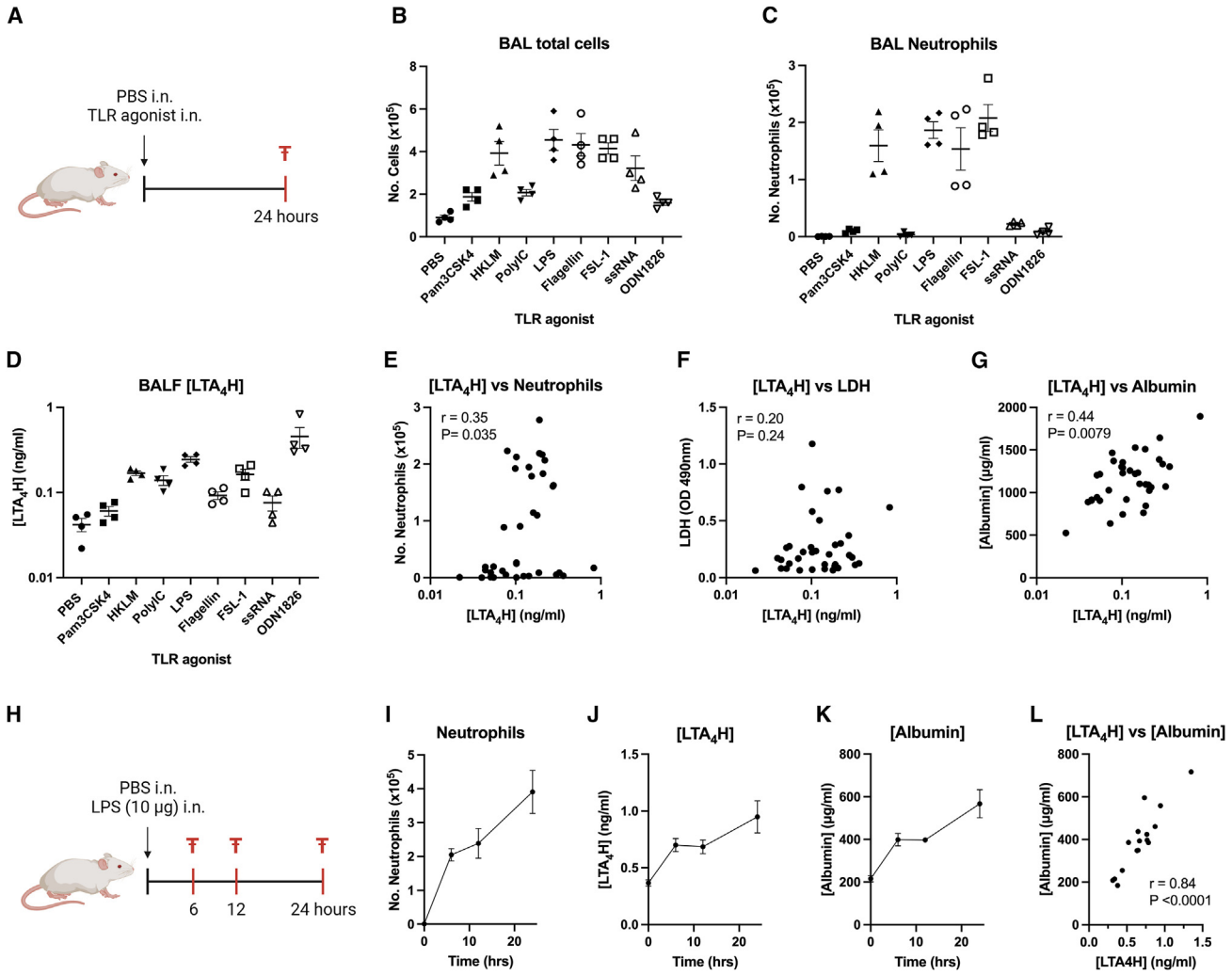

Figure 1. Extracellular airway concentrations of LTA_4H correlate with concentrations of albumin

(A) Female Balb/c mice were intranasally (i.n.) administered PBS or TLR agonists synthetic triacylated lipopeptide (1 µg), heat-killed *Listeria monocytogenes* (1×10^8), polyinosine-polycytidylic acid (50 µg), LPS (10 µg), flagellin (1 µg), synthetic diacylated lipoprotein (1 µg), single-stranded RNA (2.5 µg), or CpG oligonucleotide (10 µg). At 24 h after i.n. administration, bronchoalveolar lavage fluid (BALF) was collected (Ŧ).

(B) Total cell numbers in the airways were assessed by trypan blue exclusion.

(C) Total numbers of neutrophils in the airways were determined by flow cytometry.

(D) Concentrations of extracellular LTA_4H in the BALF were determined by ELISA.

(E–G) BALF LTA_4H concentrations were correlated with airway neutrophil numbers (E), BALF LDH activity as a surrogate for cell death (F), and concentrations of albumin in the BALF (G).

(H) Female Balb/c mice were i.n. administered PBS or LPS (10 µg). At 6-, 12-, and 24-h time points after i.n. administration, BALF was collected (Ŧ).

(I) Total numbers of neutrophils in the airways were determined by flow cytometry.

(J and K) Concentrations of extracellular LTA_4H (J) and albumin (K) in the BALF were determined by ELISA.

(L) BALF LTA_4H concentrations were correlated with BALF concentrations of albumin. Figures are representative of 2 independent experiments with 4–6 mice per group in each experiment. Results are depicted as mean ± SEM. Correlation analysis was performed using a Spearman rank test.

albumin concentrations. Furthermore, neutrophil depletion in MIP-2 treated mice, by administration of anti-Ly6G antibody (1A8), abrogated chemokine-induced elevations in airway albumin and LTA_4H activity (Figure S1). Thus, elevated extracellular LTA_4H seen to previously coincide with neutrophilic infiltrate may reflect changes in vascular permeability attributed to the neutrophil rather than specific release of LTA_4H from the neutrophil.

It was next questioned whether agents that induced changes in vascular permeability without eliciting airway neutrophilic inflammation could also drive increased BALF LTA_4H concentrations. Accordingly, administration of histamine to mice (Figure 4A) did not result in increased total airway cellularity (Figure 4B) or airway neutrophils (Figure 4C) but did give rise to significant elevations in BALF concentrations of albumin (Figure 4D), LTA_4H (Figure 4E), and BALF PGP-degrading activity (Figure 4F). BALF LTA_4H

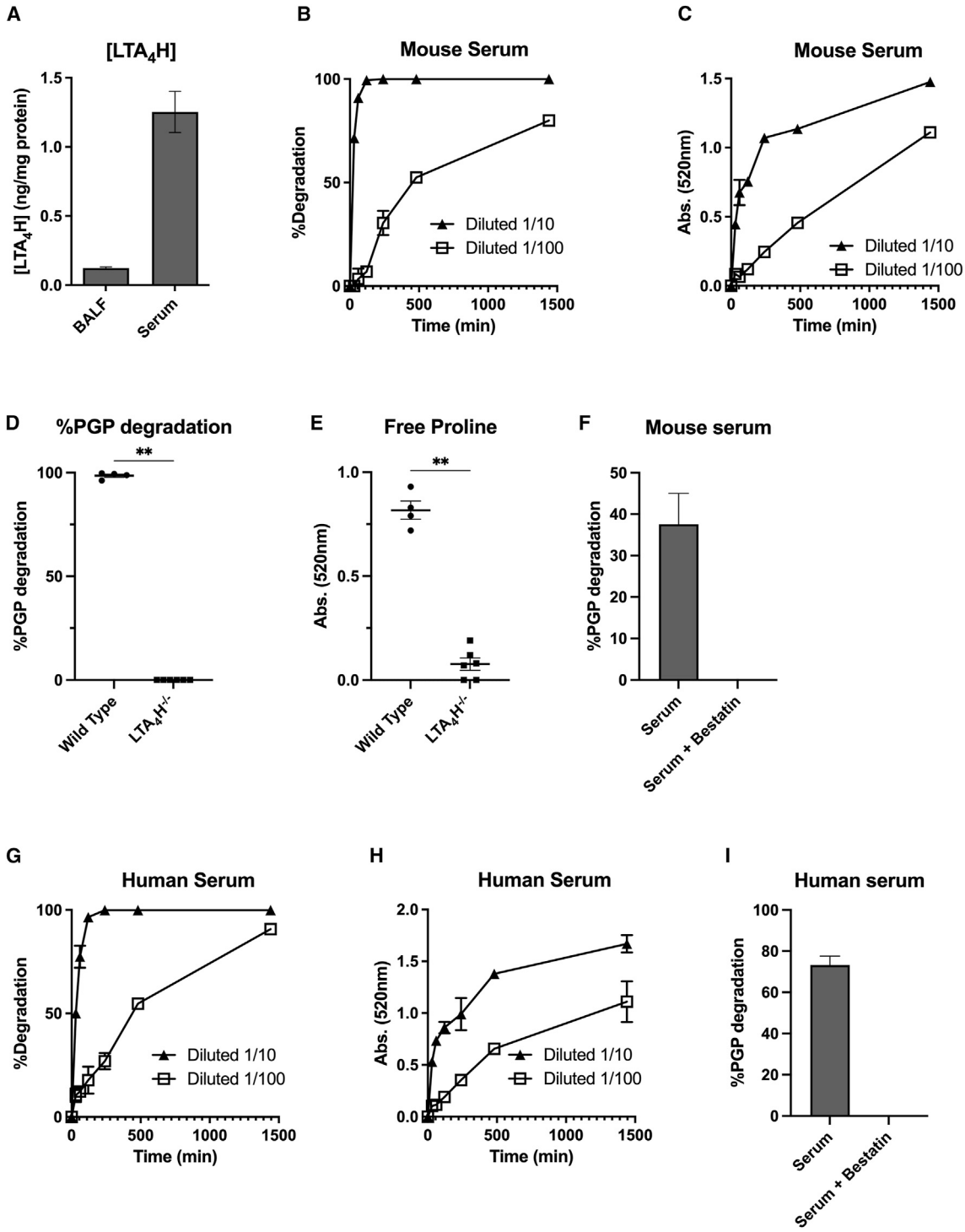

Figure 2. Serum is an abundant source of extracellular LTA_4H with robust PGP-degrading activity

(A) Concentrations of LTA_4H in BALF and serum of naive, female Balb/c mice, as determined by ELISA and expressed as nanograms (ng) of LTA_4H per milligram (mg) of total protein.

(B and C) Naive, female Balb/c mouse serum was diluted 1/10 or 1/100 and incubated with PGP (final concentration 100 μg/mL) at 37°C for varying lengths of time. At each time point, PGP degradation was assessed by measuring loss of peptide by mass spectrometry (B; expressed as percentage degradation relative to peptide alone) and ensuing liberation of free proline and its reaction with ninhydrin (C).

(legend continued on next page)

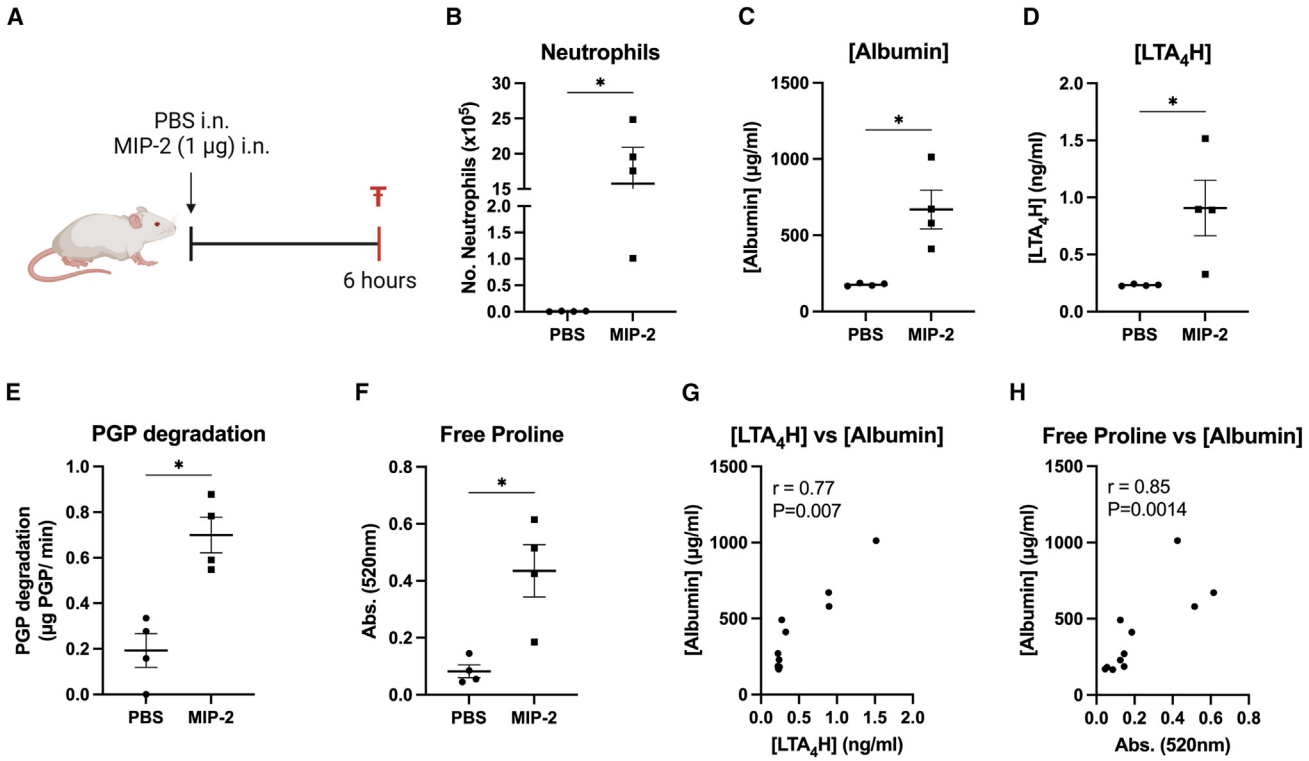

Figure 3. Airway extracellular LTA_4H concentrations are augmented during neutrophilic inflammation

(A) Female Balb/c mice were intranasally (i.n.) administered PBS or MIP-2 (1 µg), and bronchoalveolar lavage fluid (BALF) was collected after 6 h (Ŧ).

(B) Total numbers of neutrophils in the airways were determined by flow cytometry.

(C and D) Concentrations of albumin (C) and extracellular LTA_4H (D) in the BALF were determined by ELISA.

(E and F) BALF obtained from PBS/MIP-2-exposed mice was diluted 1/10 and incubated with PGP (final concentration 100 µg/mL) at 37°C for 2 h. PGP degradation was assessed by measuring loss of peptide by mass spectrometry (E; expressed as percentage degradation relative to peptide alone) and ensuing liberation of free proline and its reaction with ninhydrin (F).

(G) BALF LTA_4H concentrations were correlated with BALF concentrations of albumin.

(H) BALF LTA_4H activity, as adjudged by liberation of free proline, was correlated with BALF concentrations of albumin. Figures are representative of 2 independent experiments with 4–6 mice per group in each experiment. Results are depicted as mean ± SEM. *$p < 0.05$ using Mann-Whitney statistical test. Correlation analysis was performed using a Spearman rank test. See also Figure S1.

concentrations (Figure 4G) and PGP-degrading activity (Figure 4H) once again displayed a significant correlation with BALF albumin concentrations. Finally, an anti-CD144 (VE-cadherin) antibody was administered to mice to destabilize endothelial junctions (Figure 4I), as previously reported.[23] Administration of anti-CD144 antibody did not increase airway neutrophilic infiltrate (Figure 4J) but did augment concentrations of albumin (Figure 4K) and LTA_4H (Figure 4L) in BALF and BALF PGP-degrading activity (Figure 4M). Airway LTA_4H concentrations (Figure 4N) and PGP-degrading activity (Figure 4O) once again significantly correlated with BALF albumin concentrations. Collectively, these analyses indicate that elevations in extracellular BALF LTA_4H manifest because of changes in vascular permeability and incursion of blood LTA_4H into the lung and airways.

(D and E) Serum obtained from naive $LTA_4H^{-/-}$ mice and littermate controls (wild type), on a 129/S2 background, were diluted 1/10 and incubated with PGP (final concentration 100 µg/mL) at 37°C for 30 min. PGP degradation was assessed by measuring loss of peptide by mass spectrometry (D; expressed as percentage degradation relative to peptide alone) and ensuing liberation of free proline and its reaction with ninhydrin (E).

(F) Serum from naive, female Balb/c mice was diluted 1/10 and incubated with PGP (final concentration 100 µg/mL) at 37°C for 30 min in the presence of bestatin (1 mM) or vehicle control. PGP degradation was assessed by measuring loss of peptide by mass spectrometry (expressed as percentage degradation relative to peptide alone).

(G and H) Serum obtained from peripheral blood of healthy volunteers was diluted 1/10 or 1/100 and incubated with PGP (final concentration 100 µg/mL) at 37°C for varying lengths of time. At each time point, PGP degradation was assessed by measuring loss of peptide by mass spectrometry (G; expressed as percentage degradation relative to peptide alone) and ensuing liberation of free proline and its reaction with ninhydrin (H).

(I) Serum peripheral blood of healthy volunteers was diluted 1/10 and incubated with PGP (final concentration 100 µg/mL) at 37°C for 30 min in the presence of bestatin (1 mM) or vehicle control. PGP degradation was assessed by measuring loss of peptide by mass spectrometry (expressed as percentage degradation relative to peptide alone). Data (mean ± SD for B, C, and F–I; mean ± SEM for A, D, and E) are representative of two experiments with $n \geq 2$ replicates (B, C, and F–I) or two of 2 independent experiments with 4–6 mice per group in each experiment (A, D, and E). **$p < 0.01$ using Mann-Whitney statistical test.

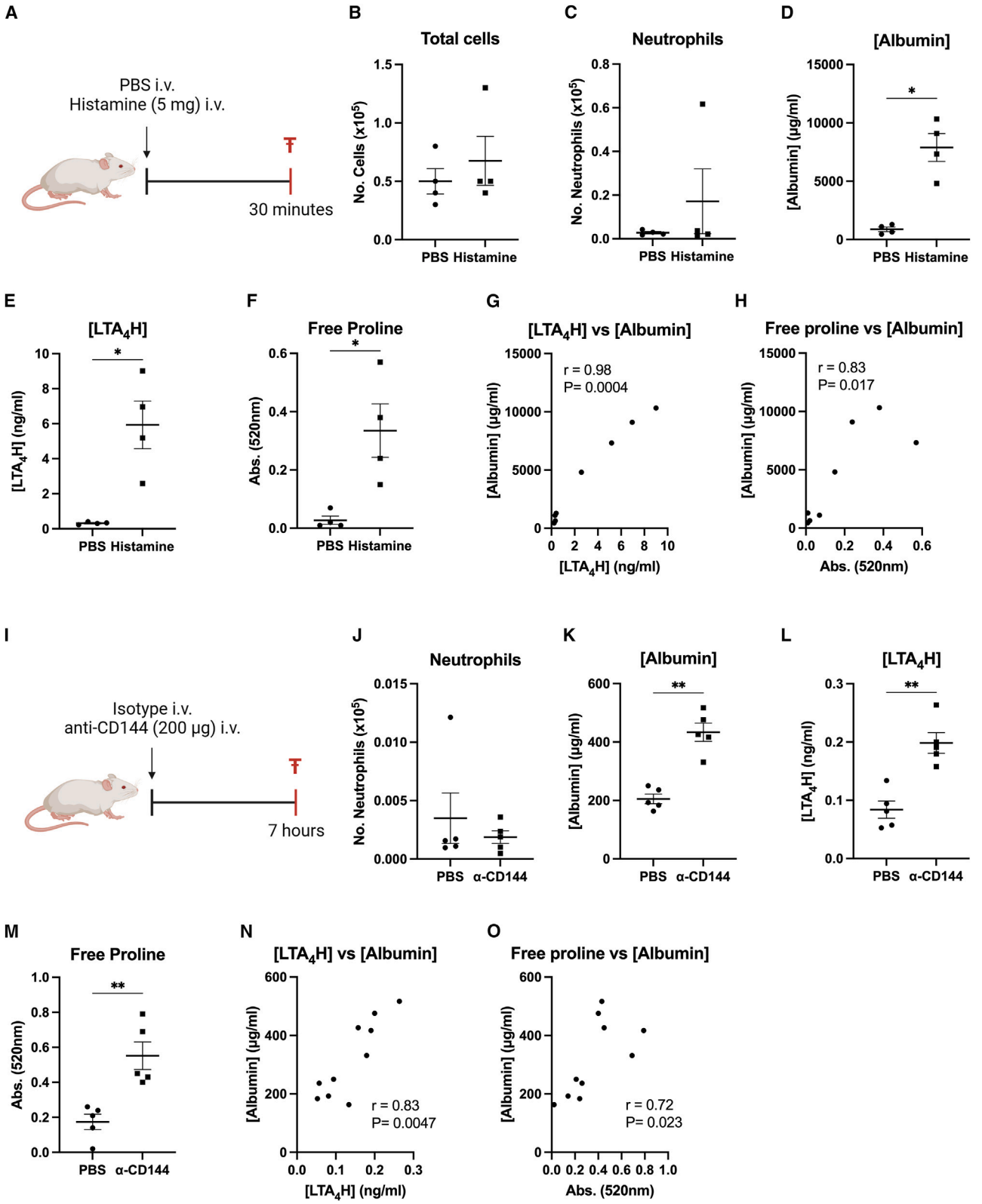

(legend on next page)

Immune cells are not a significant contributor to serum extracellular LTA_4H

The cellular source of the substantial concentrations of extracellular LTA_4H in the blood was subsequently questioned. Within the cellular components of human blood, polymorphonuclear neutrophils (PMNs), peripheral blood mononuclear cells (PBMCs), and, to a lesser extent, red blood cells (RBCs) all expressed LTA_4H, as adjudged by western blot (Figure 5A). Subsequently, cell lysates and supernatants from cultured, unstimulated PMNs, PBMCs, and RBCs were assessed for their capacity to degrade PGP to infer whether they spontaneously secrete LTA_4H without provocation and could account for high serum LTA_4H concentrations. While PGP-degrading activity was readily detectable in lysate of PMNs, PBMCs, and RBCs, activity was minimal in cell supernatants (Figures 5B–5D), suggesting there is minimal constitutive release of LTA_4H; although, some activity was detectable in PMN supernatants (Figure 5B). However, neutrophils are unlikely to be significant contributors to serum repositories of LTA_4H, as neutrophil depletion in mice using the highly selective anti-Ly6G antibody (1A8)[24,25] (Figure 5E) failed to reduce serum LTA_4H concentrations (Figure 5F) or PGP-degrading activity (Figure 5G). This 1A8 dosing protocol was based on extensive prior optimization that yielded complete and specific ablation of blood neutrophil numbers[24] (Figure S2A) while causing no detectable increase in liver injury (Figure S2B). Subsequently, blood of naive mice was separated into plasma and cellular components, and each were assessed for relative concentrations of LTA_4H. When LTA_4H concentrations were expressed per milligram of total protein, levels were substantially greater in plasma than cell lysate (Figure 5H), suggesting that even large-scale cell lysis would be insufficient to account for the substantial extracellular blood LTA_4H concentrations. When absolute concentrations of LTA_4H in plasma and cellular components of a milliliter of blood were enumerated, levels were again significantly greater in plasma (Figure 5I); thus, even if hematopoietic cells selectively released all of their intracellular LTA_4H, it would still be insufficient to account for concentrations found in plasma. Combined, these analyses suggest that the large repositories of extracellular LTA_4H in the blood are unlikely to originate from hematopoietic cells.

Liver hepatocytes release LTA_4H, with secretion augmented in response to acute phase stimulants

A large proportion of serum proteins originate from the liver, and thus, it was questioned whether this organ could represent a major source of extracellular LTA_4H. Significant concentrations of LTA_4H were present in liver homogenate of naive mice, being significantly enriched compared to serum levels (Figure 6A). Accordingly, LTA_4H was detectable in livers of wild-type naive mice, as determined by western blot, but not in *Lta4h*$^{-/-}$ animals (Figure 6B). Substantial PGP-degrading activity was detectable in liver homogenates of wild-type naive mice but absent in *Lta4h*$^{-/-}$ animals, again demonstrating the lack of redundancy in PGP-degrading machinery (Figures 6C and 6D). Immunohistochemistry analysis of mouse liver tissue demonstrated that LTA_4H was broadly expressed in hepatocytes, the liver cells responsible for generating and secreting most of the plasma proteins (Figure 6E).

The human HepG2 hepatocyte cell line also expressed LTA_4H, as adjudged by western blot (Figure 6F). Despite the abundance of intracellular LTA_4H in hepatocytes, they were unable to perform the archetypical intracellular function of this enzyme in generating LTB_4, in stark contrast to neutrophils (Figure 6G). It was rationalized that the abundance of LTA_4H was instead destined for release to perform its secondary extracellular function. Accordingly, HepG2 cells constitutively released LTA_4H, which had capacity to degrade PGP (Figure 6H). LTA_4H lacks a classical signal peptide for release via a conventional protein secretion pathway. Intriguingly, release of LTA_4H from HepG2 cells was unaffected by the presence of brefeldin A, potentially suggesting that release of the enzyme could be via an unconventional protein secretion pathway (Figure 6I). While LTA_4H is constitutively released from HepG2 cells, it was found that inflammatory cytokines known to elicit an acute phase response, specifically interleukin-6 (IL-6) and IL-1β, markedly increased release of the enzyme (Figures 6J and 6K). Importantly, changes in PGP-degrading activity in HepG2 supernatants were independent of cell death (Figures S3A and S3B).

We next sought to ascertain whether comparable findings could be obtained from primary hepatocytes. Accordingly, LTA_4H was demonstrated to be present in lysate of isolated

Figure 4. Airway extracellular LTA_4H concentrations are defined by the level of vascular permeability

(A) Female Balb/c mice were intravenously (i.v.) administered PBS or histamine (5 mg), and bronchoalveolar lavage fluid (BALF) was collected after 30 min (Ŧ).
(B) Total cell numbers in the airways were assessed by trypan blue exclusion.
(C) Total numbers of neutrophils in the airways were determined by flow cytometry.
(D and E) Concentrations of albumin (D) and extracellular LTA_4H (E) in the BALF were determined by ELISA.
(F) BALF obtained from PBS/histamine-exposed mice was diluted 1/10 and incubated with PGP (final concentration 100 μg/mL) at 37°C for 2 h. PGP degradation was assessed by measuring liberation of free proline and its reaction with ninhydrin.
(G) BALF LTA_4H concentrations were correlated with BALF concentrations of albumin.
(H) BALF LTA_4H activity, as adjudged by liberation of free proline, was correlated with BALF concentrations of albumin.
(I) Female Balb/c mice were i.v. administered isotype control or anti-CD144 antibody (200 μg), and bronchoalveolar lavage fluid (BALF) was collected after 7 h (Ŧ).
(J) Total numbers of neutrophils in the airways were determined by flow cytometry.
(K and L) Concentrations of albumin (K) and extracellular LTA_4H (L) in the BALF were determined by ELISA.
(M) BALF obtained from anti-CD144 antibody/isotype control antibody treated mice was diluted 1/10 and incubated with PGP (final concentration 100 μg/mL) at 37°C for 2 h. PGP degradation was assessed by measuring liberation of free proline and its reaction with ninhydrin.
(N) BALF LTA_4H concentrations were correlated with BALF concentrations of albumin.
(O) BALF LTA_4H activity, as adjudged by liberation of free proline, was correlated with BALF concentrations of albumin. Figures are representative of 2 independent experiments with 4–6 mice per group in each experiment. Results are depicted as mean ± SEM. *$p < 0.05$, **$p < 0.01$ using Mann-Whitney statistical test. Correlation analysis was performed using a Spearman rank test.

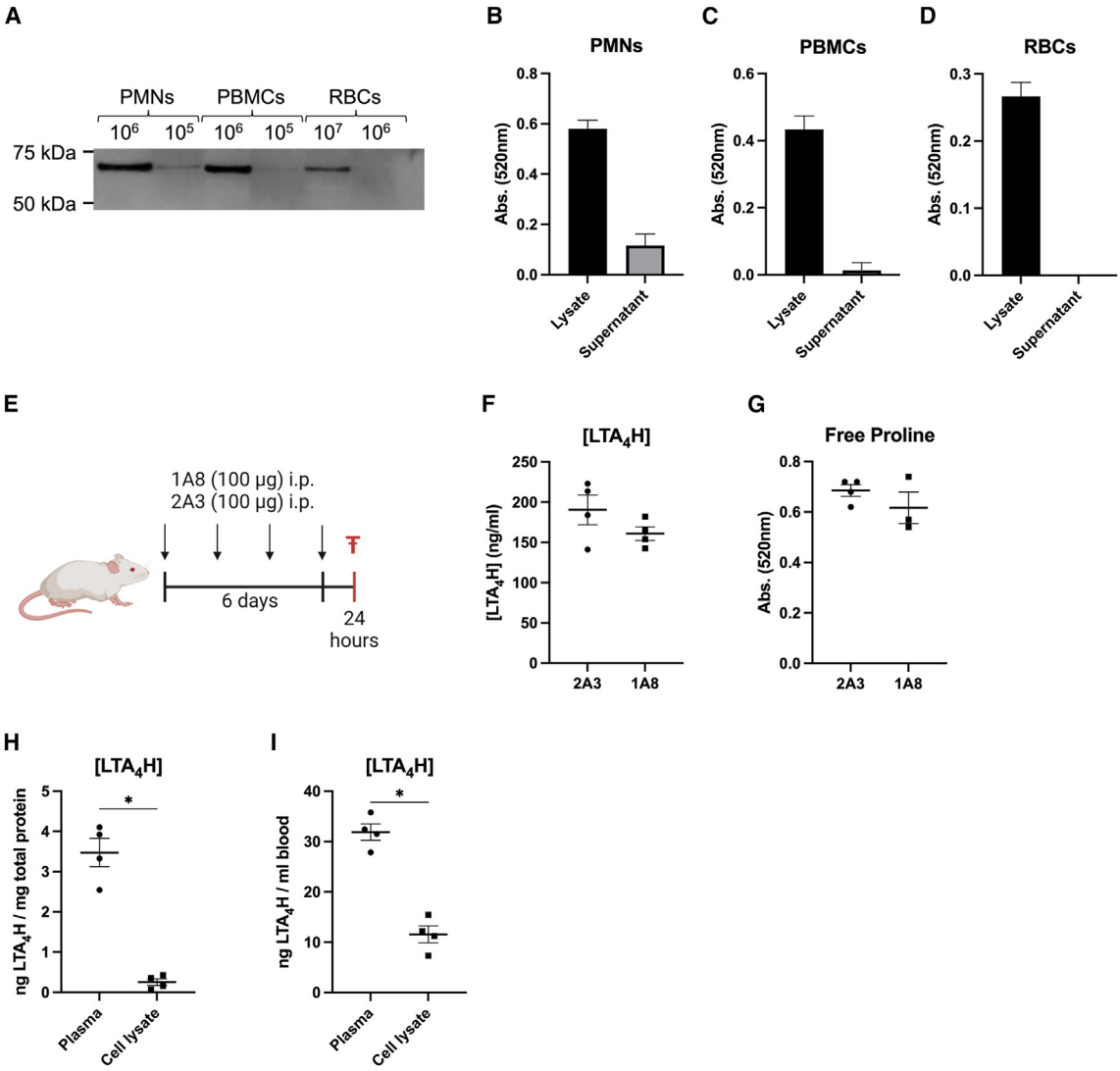

Figure 5. Immune cells are not a significant contributor to serum extracellular LTA_4H

(A) Polymorphonuclear neutrophils (PMNs; 1×10^5 and 1×10^6 cells), peripheral blood mononuclear cells (PBMCs; 1×10^5 and 1×10^6 cells), and red blood cells (RBCs; 1×10^6 and 1×10^7 cells) were isolated from peripheral blood of healthy volunteers and subjected to a western blot for LTA_4H.

(B–D) Lysates and supernatants were obtained from PMNs (B; 2×10^5 cells), PBMCs (C; 2×10^5 cells), and RBCs (D; 2×10^7 cells) cultured for 6 h in serum-free media. Cell lysates (diluted 1/10) and supernatants were incubated with PGP (final concentration 100 µg/mL) at 37°C for 2 h. PGP degradation was assessed by measuring liberation of free proline and its reaction with ninhydrin.

(E) Female Balb/c mice were intraperitoneally (i.p.) administered 100 µg neutrophil-depleting antibody (1A8) or isotype control antibody (2A3) on alternate days for a period of 1 week, and blood was extracted 24 h after the last dose of antibody.

(F) Serum concentrations of LTA_4H were determined by ELISA.

(G) Serum from control and neutrophil-depleted mice were diluted 1/10 and incubated with PGP (final concentration 100 µg/mL) at 37°C for 30 min. PGP degradation was assessed by liberation of free proline and its reaction with ninhydrin.

(H and I) Blood was extracted from naive Balb/c mice and separated into plasma and cellular constituents. Concentrations of LTA_4H in the plasma and cell lysate were determined by ELISA and are expressed at nanograms of enzyme per milligram of total protein (H) and nanograms of enzyme per milliliter of blood (I). Data (mean ± SD for B–D; mean ± SEM for F–I) are representative of two experiments with triplicates (B–D) or two of 2 independent experiments with 4–6 mice per group in each experiment (F–I). *$p < 0.05$ using Mann-Whitney statistical test. See also Figure S2.

primary mouse hepatocytes (PMHs), as adjudged by western blot (Figure 6L). Once again, primary hepatocytes constitutively released LTA_4H (Figure 6M), and release was unaffected by incubation with brefeldin A (Figure 6N). Moreover, LTA_4H release from PMHs was increased following incubation with IL-1β (Figure 6O), independent of changes to cell death (Figure S3C). Recapitulating these findings *in vivo*, induction of an acute phase response in mice by IL-1β administration (Figure 6P) resulted in a significant increase in LTA_4H concentrations in the liver (Figure 6Q) and serum (Figure 6R).

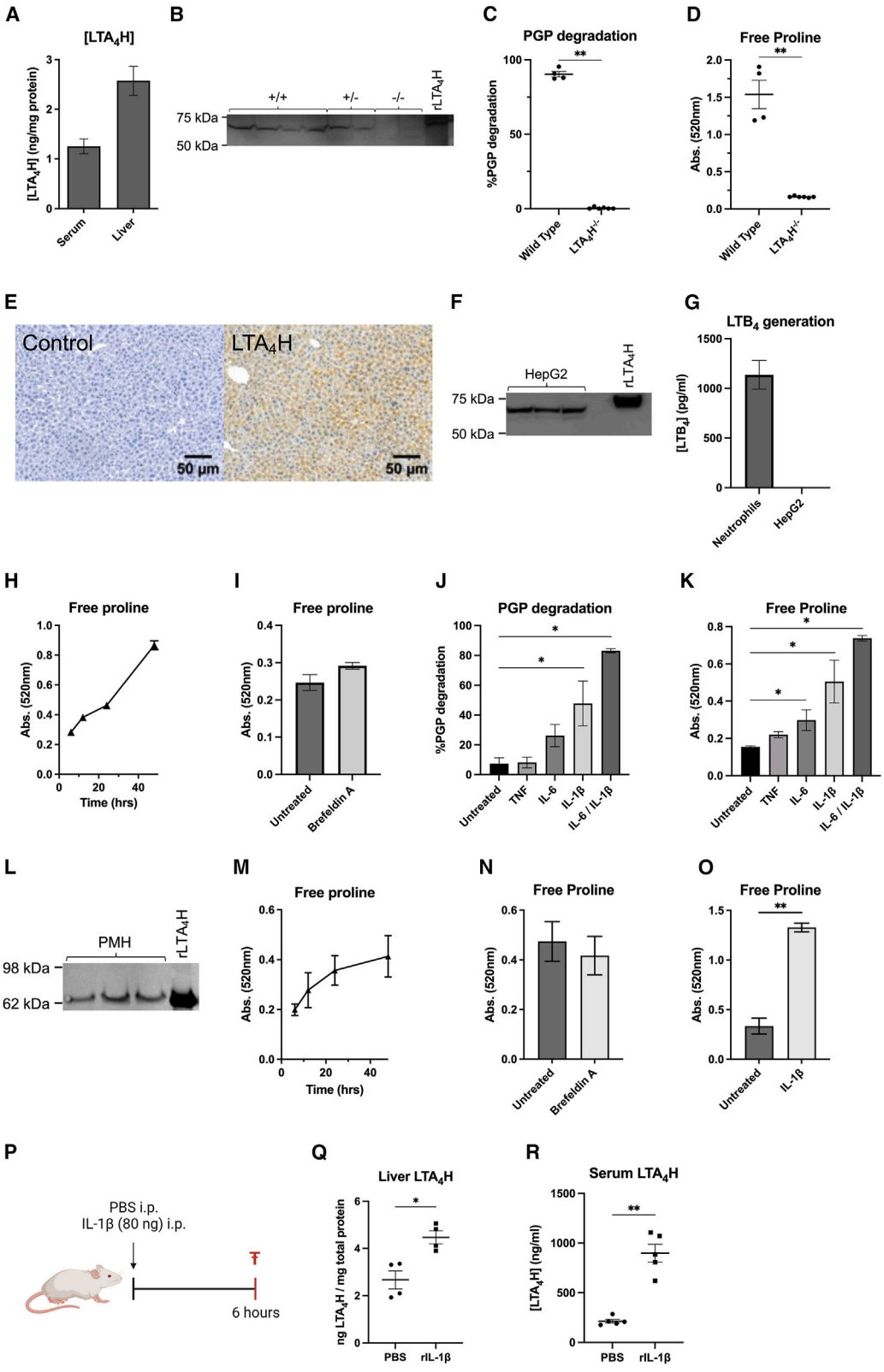

(legend on next page)

DISCUSSION

In this study, we have interrogated the previously undefined pathways that govern the bioavailability of extracellular LTA_4H. We demonstrate that airway extracellular LTA_4H concentrations are defined by the level of pulmonary vascular permeability and the ensuing influx of enzyme from the abundant repository within the blood. In turn, liver hepatocytes are a significant source of blood-borne LTA_4H, whereby they constitutively release the enzyme, with production further increased as part of an acute phase response. Thus, airway concentrations of extracellular LTA_4H are dictated locally at the level of tissue vascular permeability and systemically by the extent of release from liver hepatocytes (Figure 7).

It makes sense that high concentrations of extracellular LTA_4H constitutively reside in the blood to ensure rapid clearance of tissue extracellular matrix (ECM)-derived PGP and prevent adverse consequences that may arise from its systemic accumulation and persistence. Albumin bears an intimate relationship with LTA_4H, whereby it binds to the enzyme and selectively boosts its aminopeptidase activity.[11,26] A constitutive pool of highly active LTA_4H is therefore present and primed to degrade PGP in the blood, and albumin and LTA_4H subsequently display coordinated infiltration of inflamed lung tissue secondary to changes in vascular permeability—an association facilitated by their virtually identical sizes. Most studies interrogating LTA_4H expression have evaluated its location intracellularly. While some studies have reported the presence of extracellular LTA_4H, or LTA_4H-like activity, in the blood, there has been limited consideration of its functional implications.[27–29]

Previous studies demonstrated that airway neutrophilic infiltration during acute inflammatory episodes coincided with release of PGP-generating enzymes (MMP-9 and PE) and liberation of PGP from collagen.[10,11] Neutrophils are an abundant source of MMP-9 and PE, and it has been rationalized that this is a pathway whereby they propagate their numbers.[13,14,30,31] However, neutrophil accumulation also coincided with a concomitant increase in extracellular LTA_4H that is critical for PGP degradation and resolution of neutrophilic inflammation. Neutrophils express LTA_4H intracellularly (to generate LTB_4), and depletion of neutrophils in acute inflammatory models has resulted in a reduction in extracellular LTA_4H concentrations[10]; thus, it was rationalized that neutrophils were a primary source of extracellular LTA_4H. However, we now demonstrate that neutrophils indirectly facilitate elevations in extracellular airway LTA_4H by promoting vascular permeability and enabling influx of enzyme from the blood. Neutrophils can potentiate increases in vascular permeability, and stimulation of neutrophils with various chemoattractants (including LTB_4) induces microvascular leakage through the release of tumor necrosis factor (TNF).[22] Thus, neutrophils not only promote their own inflammation through PGP generation but also then indirectly facilitate PGP degradation to enable inflammatory resolution and limit neutrophil-mediated pathology. However, neutrophils are not a

Figure 6. Liver hepatocytes express substantial quantities of LTA_4H, with secretion augmented in response to acute phase stimulants

(A) Concentrations of LTA_4H in serum and liver homogenate of naive, female Balb/c mice, as determined by ELISA and expressed as nanograms (ng) of LTA_4H per milligram (mg) of total protein.

(B) Western blot for LTA_4H in liver homogenate of $LTA_4H^{+/+}$ (wild type), $LTA_4H^{+/-}$ (heterozygote), and $LTA_4H^{-/-}$ (knockout) mice.

(C and D) Serum obtained from naive $LTA_4H^{-/-}$ mice and littermate controls (wild type), on a 129/S background, were diluted 1/100 and incubated with PGP (final concentration 100 μg/mL) at 37°C for 1 h. PGP degradation was assessed by measuring loss of peptide by mass spectrometry (C; expressed as percentage degradation relative to peptide alone) and ensuing liberation of free proline and its reaction with ninhydrin (D).

(E) Immunohistochemistry of liver slices derived from naive female Balb/c mice that have been stained with isotype control antibody or antibody to LTA_4H. Brown coloration depicts positive staining for LTA_4H, and blue is hematoxylin counterstain.

(F) Western blot for LTA_4H in human hepatocyte cell line HepG2s.

(G) LTB_4 generation by human peripheral blood neutrophils and HepG2 cells, as adjudged by ELISA, following stimulation with calcium ionophore A23187.

(H) Supernatants were collected from cultured, unstimulated HepG2 cells at distinct time points for assessment of release of PGP-degrading LTA_4H. HepG2 supernatants were diluted 1/10 and incubated with PGP (final concentration 100 μg/mL) at 37°C for 2 h. PGP degradation was assessed by measuring liberation of free proline and its reaction with ninhydrin.

(I) HepG2 cells were cultured for 12 h in media alone or media supplemented with brefeldin A (10 μg/mL). HepG2 supernatants were diluted 1/10 and incubated with PGP (final concentration 100 μg/mL) at 37°C for 2 h. PGP degradation was assessed by measuring liberation of free proline and its reaction with ninhydrin.

(J and K) HepG2 cells were cultured for 12 h in media alone or media supplemented with TNF (10 ng/mL), IL-6 (10 ng/mL), IL-1β (1 ng/mL), or IL-6 and IL-1β. HepG2 supernatants were diluted 1/10 and incubated with PGP (final concentration 100 μg/mL) at 37°C for 2 h. PGP degradation was assessed by measuring loss of peptide by mass spectrometry (J; expressed as percentage degradation relative to peptide alone) and ensuing liberation of free proline and its reaction with ninhydrin (K).

(L) Western blot for LTA_4H in primary mouse hepatocyte (PMH) cell lysate.

(M) Supernatants were collected from cultures of unstimulated primary mouse hepatocytes at distinct time points for assessment of release of PGP-degrading LTA_4H. Supernatants were incubated with PGP (final concentration 100 μg/mL) at 37°C for 2 h. PGP degradation was assessed by measuring liberation of free proline and its reaction with ninhydrin.

(N) Primary mouse hepatocytes were cultured for 12 h in media alone or media supplemented with brefeldin A (10 μg/mL). Supernatants were incubated with PGP (final concentration 100 μg/mL) at 37°C for 2 h. PGP degradation was assessed by measuring liberation of free proline and its reaction with ninhydrin.

(O) Primary mouse hepatocytes were cultured for 12 h in media alone or media supplemented with IL-1β (1 ng/mL). Supernatants were incubated with PGP (final concentration 100 μg/mL) at 37°C for 2 h. PGP degradation was assessed by measuring liberation of free proline and its reaction with ninhydrin.

(P) Female Balb/c mice were intraperitoneally (i.p.) administered 80 ng of IL-1β or vehicle control, and blood and liver were extracted 6 h later.

(Q and R) Concentrations of LTA_4H were determined by ELISA in liver homogenate (Q; expressed per mg of total protein) and serum (R). Results are depicted as mean ± SEM for (A), (D), (E), (Q), and (L) and mean ± SD for (G)–(K) and (M)–(O). Data are representative of two experiments with $n \geq 3$ replicates (G–K and N), 1 experiment with $n = 6$ replicates (M and O), or 2 independent experiments with 4–6 mice per group in each experiment (Q and R). $^*p < 0.05$, $^{**}p < 0.01$ using Mann-Whitney statistical test. See also Figure S3.

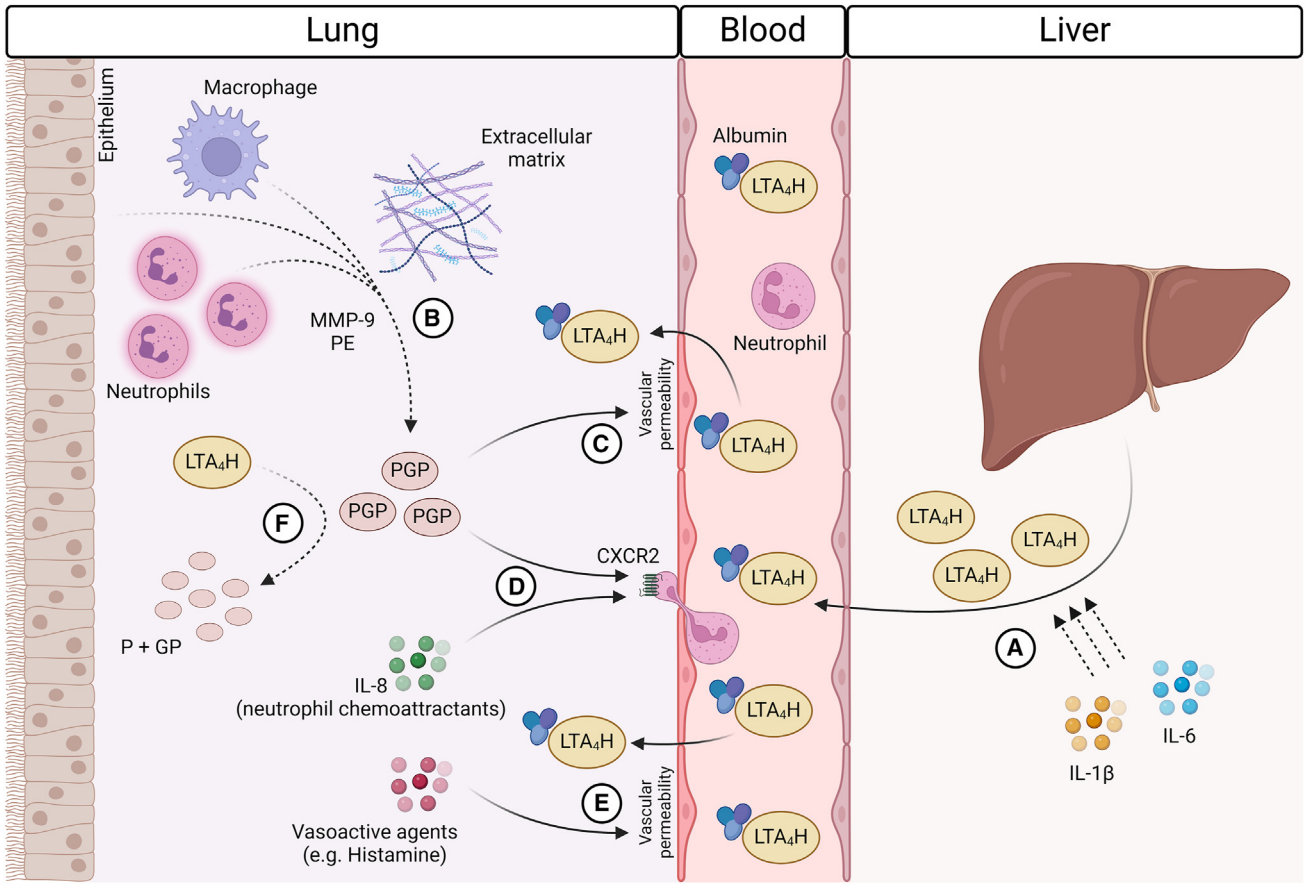

Figure 7. Proposed mechanism defining the bioavailability of extracellular LTA_4H in the lung

(A) Liver hepatocytes constitutively release LTA_4H extracellularly into the bloodstream, with synthesis and release being augmented by acute phase stimulants IL-6 and IL-1β. Within the blood, extracellular LTA_4H binds albumin, which functions to augment its PGP-degrading activity.

(B) In response to infection or injury of the lung, resident and recruited cells (encompassing macrophages, epithelial cells, and neutrophils) release PGP-generating enzymes matrix metalloproteinase-9 (MMP-9) and prolyl endopeptidase (PE). These enzymes operate sequentially to generate the bioactive tripeptide proline-glycine-proline (PGP) from collagen of the extracellular matrix. PGP operates to promote epithelial repair and neutrophil recruitment to sterilize the site.

(C) PGP is able to act directly on endothelial cells to promote vascular permeability and enable blood-borne extracellular LTA_4H to move into the lung tissue.

(D) Neutrophils recruited from the vasculature into the lung in response to liberated PGP, or other neutrophil chemoattractants, induce vascular permeability during extravasation, enabling extracellular LTA_4H to move from the bloodstream into the lung tissue.

(E) Vasoactive agents released locally within the lung (such as histamine) are also able to act directly on endothelial cells to promote vascular permeability and enable influx of extracellular LTA_4H from the blood.

(F) Extracellular LTA_4H that has moved from the blood stream into the lung is able to efficiently degrade PGP to prevent its accumulation and persistence and ensuing pathological sequelae.

pre-requisite for PGP generation nor for vascular changes that allow influx of extracellular LTA_4H into the airways. PGP-generating enzymes can be released from a variety of cells,[32–34] and we have demonstrated that vasoactive agents can potentiate neutrophil-independent accumulation of extracellular airway LTA_4H. ECM collagen contributes to endothelial barrier function, and MMPs central to PGP generation can augment endothelial permeability[21,35]—thus facilitating degradation of the peptide they generate. PGP itself has also been shown to promote endothelial permeability,[36] thus indirectly acting to limit its own bioavailability. Thus, PGP is generated in response to lung injury or infection and subsequently operates to facilitate sterilization and repair of the site. However, the cells/machinery that generate PGP or the peptide itself then operate to augment extracellular LTA_4H to prevent undesirable pathological consequences of PGP persistence.

We rationalize that most extracellular serum LTA_4H is derived from liver hepatocytes. Hepatocytes are a vast repository of LTA_4H and yet lack the capacity to perform the classical function of the enzyme in generating LTB_4, likely attributable to an absence of enzymes upstream of LTA_4H in the LTB_4 biosynthetic pathway that are primarily restricted to myeloid cells.[3,6] We argue that the abundance of LTA_4H within the liver is to support the secondary function of LTA_4H, whereby it is secreted extracellularly to degrade PGP. Many plasma proteins are generated by hepatocytes and constitutively released into the bloodstream to promote innate immunity, with their production enhanced as part of an acute phase response to protect the host. However,

hepatocytes also release proteins that exhibit anti-inflammatory or inhibitory roles to protect the host from overwhelming and unnecessary inflammation.[37] Alpha-1-antitrypsin is released from hepatocytes into the bloodstream and operates to suppress neutrophilic recruitment and protease activity in distal sites to temper the pathological capacity of these cells.[38] We envision that LTA_4H operates in an analogous manner to restrict PGP-mediated pathology—with activity being potentiated by liver derived albumin. LTA_4H lacks the signal peptide required for release via the classical endoplasmic reticulum/Golgi protein secretion pathway. Given our findings that brefeldin A, an inhibitor of protein transport along the classical secretory pathway, does not abrogate LTA_4H release from hepatocytes, it is possible that LTA_4H could be released to an extracellular environment as a consequence of unconventional protein secretion (UPS).[39,40]

Given that local tissue and systemic factors define the PGP-LTA_4H axis, both should be considered when evaluating how perturbations of this axis may manifest in PGP persistence and ensuing pathology. PGP is elevated in the airways of patients with CLDs such as chronic obstructive pulmonary disease (COPD), severe asthma, and cystic fibrosis and subsequently implicated in persistent neutrophilia and pathological tissue remodeling.[13,14,16–18,33,41–46] The ability of PGP to persist in these settings has been attributed to local depreciations in extracellular airway LTA_4H concentrations or activity.[16–19] However, it would now seem prudent to evaluate the impact of systemic changes in LTA_4H concentrations and alterations in vascular permeability in defining airway PGP persistence. PGP can accumulate in the blood of patients with CLDs,[43,45] which would necessitate a loss in levels or activity of circulating LTA_4H. Patients with liver diseases have been demonstrated to possess aberrant plasma levels of an undefined tripeptide aminopeptidase, which bears hallmarks of LTA_4H.[47,48] Moreover, CLDs have systemic manifestations with many associated with liver dysfunction,[49–51] and thus, it seems logical to consider if hepatocyte-mediated LTA_4H synthesis or release are perturbed in these settings. Given that albumin potentiates LTA_4H aminopeptidase activity, it is also noteworthy that hypoalbuminemia is frequently observed in patients with liver disease and systemic illness.[52] Importantly, adverse outcomes in CLDs such as COPD are associated with hypoalbuminemia[53–56]; this is pertinent given that deficiency in extracellular LTA_4H activity is a hallmark feature of COPD.[18] Moreover, systemic accumulation of PGP may also contribute to extrapulmonary manifestations and comorbidities associated with these conditions, pathologies in which PGP has, in some instances, been independently implicated.[14,41,57]

In conclusion, we describe the pathways that govern the bioavailability of extracellular LTA_4H and thus dictate the persistence of PGP. We demonstrate that liver hepatocytes constitutively release LTA_4H, with production further elevated as part of an acute phase response. Subsequent airway concentrations of LTA_4H are then defined at the level of local vascular permeability. Thus, a crosstalk between the local airway environment and the systemic circulatory and hepatic systems imparts a feedback loop that operates to ensure PGP is unable to persist and drive lung pathology. These findings have implications for our understanding of how inflammation and repair are regulated and how perturbations to this system may manifest in pathologies of CLDs.

Limitations of the study

Within this study, we have provided compelling evidence that liver hepatocytes are a prominent source of extracellular LTA_4H within the blood, which subsequently gains access to the airways secondary to changes in pulmonary vascular permeability. However, we are unable to unequivocally rule out a role for other cells in contributing to extracellular LTA_4H, particularly in chronic disease states where heightened tissue pathology may manifest with augmented extracellular LTA_4H secondary to elevated cell death. Moreover, future studies should seek to further dissect the described axis in patients and establish how changes in hepatocyte LTA_4H release, serum albumin levels, and pulmonary vascular permeability dictate airway LTA_4H and PGP concentrations and tissue pathology. As described above, LTA_4H lacks the signal peptide required for release via the classical secretion pathway, and thus, the mechanisms defining hepatocyte secretion of this enzyme demand further exploration. We have demonstrated that LTA_4H release from hepatocytes is independent of cell death and resistant to treatment with brefeldin A, potentially signifying that it is an example of UPS, the mechanisms of which should be elaborated upon in the future.

STAR★METHODS

Detailed methods are provided in the online version of this paper and include the following:

- KEY RESOURCES TABLE
- RESOURCE AVAILABILITY
  - Lead contact
  - Materials availability
  - Data and code availability
- EXPERIMENTAL MODEL AND STUDY PARTICIPANT DETAILS
  - Mice
- METHOD DETAILS
  - Mouse challenge models
  - Mouse tissue isolation and processing
  - Primary mouse hepatocyte isolation
  - Primary mouse hepatocyte culture and stimulation
  - Human samples
  - HepG2 culture and stimulation
  - PGP degradation experiments
  - ESI–LC/MS/MS for PGP detection
  - Measurement of free proline
  - LTA_4H epoxide hydrolase activity and LTB_4 generation
  - Quantification of soluble mediators
  - Flow cytometry
  - Western blot
  - Immunohistochemistry of liver tissue
- QUANTIFICATION AND STATISTICAL ANALYSIS

SUPPLEMENTAL INFORMATION

Supplemental information can be found online at https://doi.org/10.1016/j.celrep.2024.114630.

ACKNOWLEDGMENTS

Manuscript version arising from this submission. R.J.S. is a Wellcome Trust Senior Research Fellow in Basic Biomedical Sciences (209458/Z/17/Z). C.M.L. is a Wellcome Senior Research Fellow in Basic Biomedical Science (107059/Z/15/Z). The authors acknowledge financial support from Imperial College London through an Imperial College Research Fellowship grant awarded to K.T.M. We thank A. Caldwell and the Center for Mass Spectrometry at King's College London for the use of equipment and technical assistance. We thank L. Lawrence for histological sectioning and staining. The graphical abstract was created with BioRender.

AUTHOR CONTRIBUTIONS

Conceptualization, K.T.M. and R.J.S.; methodology, K.T.M., A.G., J.E.B., and R.J.S.; investigation, K.T.M., S.A., D.F.P., G.F.M., and R.J.S.; writing – original draft, K.T.M. and R.J.S.; writing – review & editing, K.T.M., C.M.L., A.G., J.E.B., and R.J.S.; funding acquisition, K.T.M. and R.J.S.; supervision, R.J.S.

DECLARATION OF INTERESTS

The authors declare that they have no competing interests.

Received: February 16, 2024
Revised: July 4, 2024
Accepted: July 30, 2024
Published: August 14, 2024

REFERENCES

1. Haeggström, J.Z., Tholander, F., and Wetterholm, A. (2007). Structure and catalytic mechanisms of leukotriene A4 hydrolase. Prostaglandins Other Lipid Mediat. *83*, 198–202. https://doi.org/10.1016/j.prostaglandins.2007.01.006.
2. Funk, C.D. (2001). Prostaglandins and leukotrienes: advances in eicosanoid biology. Science *294*, 1871–1875. https://doi.org/10.1126/science.294.5548.1871.
3. Haeggström, J.Z. (2000). Structure, function, and regulation of leukotriene A4 hydrolase. Am. J. Respir. Crit. Care Med. *161*, S25–S31. https://doi.org/10.1164/ajrccm.161.supplement_1.ltta-6.
4. Haeggström, J.Z., Kull, F., Rudberg, P.C., Tholander, F., and Thunnissen, M.M.G.M. (2002). Leukotriene A4 hydrolase. Prostaglandins Other Lipid Mediat. *68–69*, 495–510. https://doi.org/10.1016/s0090-6980(02)00051-5.
5. Haeggström, J.Z. (2004). Leukotriene A4 hydrolase/aminopeptidase, the gatekeeper of chemotactic leukotriene B4 biosynthesis. J. Biol. Chem. *279*, 50639–50642. https://doi.org/10.1074/jbc.R400027200.
6. Wan, M., Tang, X., Stsiapanava, A., and Haeggström, J.Z. (2017). Biosynthesis of leukotriene B4. Semin. Immunol. *33*, 3–15. https://doi.org/10.1016/j.smim.2017.07.012.
7. Di Gennaro, A., Kenne, E., Wan, M., Soehnlein, O., Lindbom, L., and Haeggström, J.Z. (2009). Leukotriene B4-induced changes in vascular permeability are mediated by neutrophil release of heparin-binding protein (HBP/CAP37/azurocidin). FASEB J. *23*, 1750–1757. https://doi.org/10.1096/fj.08-121277.
8. Chen, X.S., Sheller, J.R., Johnson, E.N., and Funk, C.D. (1994). Role of leukotrienes revealed by targeted disruption of the 5-lipoxygenase gene. Nature *372*, 179–182. https://doi.org/10.1038/372179a0.
9. Bailie, M.B., Standiford, T.J., Laichalk, L.L., Coffey, M.J., Strieter, R., and Peters-Golden, M. (1996). Leukotriene-deficient mice manifest enhanced lethality from Klebsiella pneumonia in association with decreased alveolar macrophage phagocytic and bactericidal activities. J. Immunol. *157*, 5221–5224.
10. Akthar, S., Patel, D.F., Beale, R.C., Peiró, T., Xu, X., Gaggar, A., Jackson, P.L., Blalock, J.E., Lloyd, C.M., and Snelgrove, R.J. (2015). Matrikines are key regulators in modulating the amplitude of lung inflammation in acute pulmonary infection. Nat. Commun. *6*, 8423. https://doi.org/10.1038/ncomms9423.
11. Snelgrove, R.J., Jackson, P.L., Hardison, M.T., Noerager, B.D., Kinloch, A., Gaggar, A., Shastry, S., Rowe, S.M., Shim, Y.M., Hussell, T., and Blalock, J.E. (2010). A Critical Role for LTA4H in Limiting Chronic Pulmonary Neutrophilic Inflammation. Science *330*, 90–94. https://doi.org/10.1126/science.1190594.
12. Patel, D.F., and Snelgrove, R.J. (2018). The multifaceted roles of the matrikine Pro-Gly-Pro in pulmonary health and disease. Eur. Respir. Rev. *27*, 180017. https://doi.org/10.1183/16000617.0017-2018.
13. Gaggar, A., Jackson, P.L., Noerager, B.D., O'Reilly, P.J., McQuaid, D.B., Rowe, S.M., Clancy, J.P., and Blalock, J.E. (2008). A novel proteolytic cascade generates an extracellular matrix-derived chemoattractant in chronic neutrophilic inflammation. J. Immunol. *180*, 5662–5669. https://doi.org/10.4049/jimmunol.180.8.5662.
14. Weathington, N.M., van Houwelingen, A.H., Noerager, B.D., Jackson, P.L., Kraneveld, A.D., Galin, F.S., Folkerts, G., Nijkamp, F.P., and Blalock, J.E. (2006). A novel peptide CXCR ligand derived from extracellular matrix degradation during airway inflammation. Nat. Med. *12*, 317–323. https://doi.org/10.1038/nm1361.
15. Kwon, Y.W., Heo, S.C., Lee, T.W., Park, G.T., Yoon, J.W., Jang, I.H., Kim, S.C., Ko, H.C., Ryu, Y., Kang, H., et al. (2017). N-Acetylated Proline-Glycine-Proline Accelerates Cutaneous Wound Healing and Neovascularization by Human Endothelial Progenitor Cells. Sci. Rep. *7*, 43057. https://doi.org/10.1038/srep43057.
16. Patel, D.F., Peiró, T., Shoemark, A., Akthar, S., Walker, S.A., Grabiec, A.M., Jackson, P.L., Hussell, T., Gaggar, A., Xu, X., et al. (2018). An extracellular matrix fragment drives epithelial remodeling and airway hyperresponsiveness. Sci. Transl. Med. *10*, eaaq0693. https://doi.org/10.1126/scitranslmed.aaq0693.
17. Turnbull, A.R., Pyle, C.J., Patel, D.F., Jackson, P.L., Hilliard, T.N., Regamey, N., Tan, H.L., Brown, S., Thursfield, R., Short, C., et al. (2020). Abnormal pro-gly-pro pathway and airway neutrophilia in pediatric cystic fibrosis. J. Cyst. Fibros. *19*, 40–48. https://doi.org/10.1016/j.jcf.2019.05.017.
18. Wells, J.M., O'Reilly, P.J., Szul, T., Sullivan, D.I., Handley, G., Garrett, C., McNicholas, C.M., Roda, M.A., Miller, B.E., Tal-Singer, R., et al. (2014). An Aberrant Leukotriene A4 Hydrolase–Proline-Glycine-Proline Pathway in the Pathogenesis of Chronic Obstructive Pulmonary Disease. Am. J. Respir. Crit. Care Med. *190*, 51–61. https://doi.org/10.1164/rccm.201401-0145OC.
19. Paige, M., Wang, K., Burdick, M., Park, S., Cha, J., Jeffery, E., Sherman, N., and Shim, Y.M. (2014). Role of leukotriene A4 hydrolase aminopeptidase in the pathogenesis of emphysema. J. Immunol. *192*, 5059–5068. https://doi.org/10.4049/jimmunol.1400452.
20. Snelgrove, R.J. (2011). Leukotriene A4 hydrolase: an anti-inflammatory role for a proinflammatory enzyme. Thorax *66*, 550–551. https://doi.org/10.1136/thoraxjnl-2011-200234.
21. Claesson-Welsh, L., Dejana, E., and McDonald, D.M. (2021). Permeability of the Endothelial Barrier: Identifying and Reconciling Controversies. Trends Mol. Med. *27*, 314–331. https://doi.org/10.1016/j.molmed.2020.11.006.
22. Finsterbusch, M., Voisin, M.B., Beyrau, M., Williams, T.J., and Nourshargh, S. (2014). Neutrophils recruited by chemoattractants in vivo induce microvascular plasma protein leakage through secretion of TNF. J. Exp. Med. *211*, 1307–1314. https://doi.org/10.1084/jem.20132413.
23. Corada, M., Mariotti, M., Thurston, G., Smith, K., Kunkel, R., Brockhaus, M., Lampugnani, M.G., Martin-Padura, I., Stoppacciaro, A., Ruco, L., et al. (1999). Vascular endothelial-cadherin is an important determinant of microvascular integrity in vivo. Proc. Natl. Acad. Sci. USA *96*, 9815–9820. https://doi.org/10.1073/pnas.96.17.9815.
24. Patel, D.F., Peiró, T., Bruno, N., Vuononvirta, J., Akthar, S., Puttur, F., Pyle, C.J., Suveizdytė, K., Walker, S.A., Singanayagam, A., et al. (2019). Neutrophils restrain allergic airway inflammation by limiting ILC2 function and

monocyte–dendritic cell antigen presentation. Sci. Immunol. *4*, eaax7006. https://doi.org/10.1126/sciimmunol.aax7006.

25. Daley, J.M., Thomay, A.A., Connolly, M.D., Reichner, J.S., and Albina, J.E. (2008). Use of Ly6G-specific monoclonal antibody to deplete neutrophils in mice. J. Leukoc. Biol. *83*, 64–70. https://doi.org/10.1189/jlb.0407247.

26. Orning, L., and Fitzpatrick, F.A. (1992). Albumins activate peptide hydrolysis by the bifunctional enzyme LTA4 hydrolase/aminopeptidase. Biochemistry *31*, 4218–4223. https://doi.org/10.1021/bi00132a010.

27. Fitzpatrick, F., Haeggström, J., Granström, E., and Samuelsson, B. (1983). Metabolism of leukotriene A4 by an enzyme in blood plasma: a possible leukotactic mechanism. Proc. Natl. Acad. Sci. USA *80*, 5425–5429. https://doi.org/10.1073/pnas.80.17.5425.

28. Adams, J.M., Rege, S.V., Liu, A.T., Vu, N.V., Raina, S., Kirsher, D.Y., Nguyen, A.L., Harish, R., Szoke, B., Leone, D.P., et al. (2023). Leukotriene A4 hydrolase inhibition improves age-related cognitive decline via modulation of synaptic function. Sci. Adv. *9*, eadf8764. https://doi.org/10.1126/sciadv.adf8764.

29. Ma, T.T., Cao, M.D., Yu, R.L., Shi, H.Y., Yan, W.J., Liu, J.G., Pan, C., Sun, J., Wei, Q.Y., Wang, D.Y., et al. (2020). Leukotriene A4 Hydrolase Is a Candidate Predictive Biomarker for Successful Allergen Immunotherapy. Front. Immunol. *11*, 559746. https://doi.org/10.3389/fimmu.2020.559746.

30. O'Reilly, P.J., Hardison, M.T., Jackson, P.L., Xu, X., Snelgrove, R.J., Gaggar, A., Galin, F.S., and Blalock, J.E. (2009). Neutrophils contain prolyl endopeptidase and generate the chemotactic peptide, PGP, from collagen. J. Neuroimmunol. *217*, 51–54. https://doi.org/10.1016/j.jneuroim.2009.09.020.

31. Xu, X., Jackson, P.L., Tanner, S., Hardison, M.T., Abdul Roda, M., Blalock, J.E., and Gaggar, A. (2011). A self-propagating matrix metalloprotease-9 (MMP-9) dependent cycle of chronic neutrophilic inflammation. PLoS One *6*, e15781. https://doi.org/10.1371/journal.pone.0015781.

32. Szul, T., Bratcher, P.E., Fraser, K.B., Kong, M., Tirouvanziam, R., Ingersoll, S., Sztul, E., Rangarajan, S., Blalock, J.E., Xu, X., and Gaggar, A. (2016). Toll-Like Receptor 4 Engagement Mediates Prolyl Endopeptidase Release from Airway Epithelia via Exosomes. Am. J. Respir. Cell Mol. Biol. *54*, 359–369. https://doi.org/10.1165/rcmb.2015-0108OC.

33. Braber, S., Koelink, P.J., Henricks, P.A.J., Jackson, P.L., Nijkamp, F.P., Garssen, J., Kraneveld, A.D., Blalock, J.E., and Folkerts, G. (2011). Cigarette smoke-induced lung emphysema in mice is associated with prolyl endopeptidase, an enzyme involved in collagen breakdown. Am. J. Physiol. Lung Cell Mol. Physiol. *300*, L255–L265. https://doi.org/10.1152/ajplung.00304.2010.

34. Wells, J.M., Gaggar, A., and Blalock, J.E. (2015). MMP generated matrikines. Matrix Biol. *44–46*, 122–129. https://doi.org/10.1016/j.matbio.2015.01.016.

35. Tong, Y., Bao, C., Xu, Y.Q., Tao, L., Zhou, Y., Zhuang, L., Meng, Y., Zhang, H., Xue, J., Wang, W., et al. (2021). The β3/5 Integrin-MMP9 Axis Regulates Pulmonary Inflammatory Response and Endothelial Leakage in Acute Lung Injury. J. Inflamm. Res. *14*, 5079–5094. https://doi.org/10.2147/jir.S331939.

36. Hahn, C.S., Scott, D.W., Xu, X., Roda, M.A., Payne, G.A., Wells, J.M., Viera, L., Winstead, C.J., Bratcher, P., Sparidans, R.W., et al. (2015). The matrikine N-α-PGP couples extracellular matrix fragmentation to endothelial permeability. Sci. Adv. *1*, e1500175. https://doi.org/10.1126/sciadv.1500175.

37. Zhou, Z., Xu, M.J., and Gao, B. (2016). Hepatocytes: a key cell type for innate immunity. Cell. Mol. Immunol. *13*, 301–315. https://doi.org/10.1038/cmi.2015.97.

38. Bergin, D.A., Reeves, E.P., Meleady, P., Henry, M., McElvaney, O.J., Carroll, T.P., Condron, C., Chotirmall, S.H., Clynes, M., O'Neill, S.J., and McElvaney, N.G. (2010). α-1 Antitrypsin regulates human neutrophil chemotaxis induced by soluble immune complexes and IL-8. J. Clin. Invest. *120*, 4236–4250. https://doi.org/10.1172/jci41196.

39. Nickel, W. (2010). Pathways of unconventional protein secretion. Curr. Opin. Biotechnol. *21*, 621–626. https://doi.org/10.1016/j.copbio.2010.06.004.

40. Nickel, W., and Rabouille, C. (2009). Mechanisms of regulated unconventional protein secretion. Nat. Rev. Mol. Cell Biol. *10*, 148–155. https://doi.org/10.1038/nrm2617.

41. van Houwelingen, A.H., Weathington, N.M., Verweij, V., Blalock, J.E., Nijkamp, F.P., and Folkerts, G. (2008). Induction of lung emphysema is prevented by L-arginine-threonine-arginine. FASEB J *22*, 3403–3408. https://doi.org/10.1096/fj.07-096230.

42. Hardison, M.T., Galin, F.S., Calderon, C.E., Djekic, U.V., Parker, S.B., Wille, K.M., Jackson, P.L., Oster, R.A., Young, K.R., Blalock, J.E., and Gaggar, A. (2009). The presence of a matrix-derived neutrophil chemoattractant in bronchiolitis obliterans syndrome after lung transplantation. J. Immunol. *182*, 4423–4431. https://doi.org/10.4049/jimmunol.0802457.

43. O'Reilly, P., Jackson, P.L., Noerager, B., Parker, S., Dransfield, M., Gaggar, A., and Blalock, J.E. (2009). N-alpha-PGP and PGP, potential biomarkers and therapeutic targets for COPD. Respir. Res. *10*, 38. https://doi.org/10.1186/1465-9921-10-38.

44. O'Reilly, P.J., Jackson, P.L., Wells, J.M., Dransfield, M.T., Scanlon, P.D., and Blalock, J.E. (2013). Sputum PGP is reduced by azithromycin treatment in patients with COPD and correlates with exacerbations. BMJ Open *3*, e004140. https://doi.org/10.1136/bmjopen-2013-004140.

45. Abdul Roda, M., Fernstrand, A.M., Redegeld, F.A., Blalock, J.E., Gaggar, A., and Folkerts, G. (2015). The matrikine PGP as a potential biomarker in COPD. Am. J. Physiol. Lung Cell Mol. Physiol. *308*, L1095–L1101. https://doi.org/10.1152/ajplung.00040.2015.

46. Roda, M.A., Xu, X., Abdalla, T.H., Sadik, M., Szul, T., Bratcher, P.E., Viera, L., Solomon, G.M., Wells, J.M., McNicholas, C.M., et al. (2019). Proline-Glycine-Proline Peptides Are Critical in the Development of Smoke-induced Emphysema. Am. J. Respir. Cell Mol. Biol. *61*, 560–566. https://doi.org/10.1165/rcmb.2018-0216OC.

47. Kanda, S., Nakamura, S., and Kanno, T. (1987). Clinical usefulness of serum tripeptide aminopeptidase activity in diagnosing liver diseases. Clin. Biochem. *20*, 53–56. https://doi.org/10.1016/s0009-9120(87)80098-x.

48. Kanda, S., Maekawa, M., Kohno, H., Sudo, K., Hishiki, S., Nakamura, S., and Kanno, T. (1984). Examination of the subcellular distribution of tripeptide aminopeptidase and evaluation of its clinical usefulness in human serum. Clin. Biochem. *17*, 253–257. https://doi.org/10.1016/s0009-9120(84)90167-x.

49. Narkewicz, M.R. (2023). Cystic fibrosis liver disease in the post-modulator era. Curr. Opin. Pulm. Med. *29*, 621–625. https://doi.org/10.1097/mcp.0000000000001017.

50. Minakata, Y., Ueda, H., Akamatsu, K., Kanda, M., Yanagisawa, S., Ichikawa, T., Koarai, A., Hirano, T., Sugiura, H., Matsunaga, K., and Ichinose, M. (2010). High COPD prevalence in patients with liver disease. Intern. Med. *49*, 2687–2691. https://doi.org/10.2169/internalmedicine.49.3948.

51. Viglino, D., Jullian-Desayes, I., Minoves, M., Aron-Wisnewsky, J., Leroy, V., Zarski, J.P., Tamisier, R., Joyeux-Faure, M., and Pépin, J.L. (2017). Nonalcoholic fatty liver disease in chronic obstructive pulmonary disease. Eur. Respir. J. *49*, 1601923. https://doi.org/10.1183/13993003.01923-2016.

52. Gounden, V., Vashisht, R., and Jialal, I. (2024). Hypoalbuminemia. In StatPearls Publishing Copyright © 2024 (StatPearls Publishing LLC).

53. Chen, C.W., Chen, Y.Y., Lu, C.L., Chen, S.C.C., Chen, Y.J., Lin, M.S., and Chen, W. (2015). Severe hypoalbuminemia is a strong independent risk factor for acute respiratory failure in COPD: a nationwide cohort study. Int. J. Chron. Obstruct. Pulmon. Dis. *10*, 1147–1154. https://doi.org/10.2147/copd.S85831.

54. Connors, A.F., Jr., Dawson, N.V., Thomas, C., Harrell, F.E., Jr., Desbiens, N., Fulkerson, W.J., Kussin, P., Bellamy, P., Goldman, L., and Knaus, W.A. (1996). Outcomes following acute exacerbation of severe chronic

obstructive lung disease. The SUPPORT investigators (Study to Understand Prognoses and Preferences for Outcomes and Risks of Treatments). Am. J. Respir. Crit. Care Med. *154*, 959–967. https://doi.org/10.1164/ajrccm.154.4.8887592.

55. Hasegawa, W., Yamauchi, Y., Yasunaga, H., Sunohara, M., Jo, T., Matsui, H., Fushimi, K., Takami, K., and Nagase, T. (2014). Factors affecting mortality following emergency admission for chronic obstructive pulmonary disease. BMC Pulm. Med. *14*, 151. https://doi.org/10.1186/1471-2466-14-151.

56. Haja Mydin, H., Murphy, S., Clague, H., Sridharan, K., and Taylor, I.K. (2013). Anemia and performance status as prognostic markers in acute hypercapnic respiratory failure due to chronic obstructive pulmonary disease. Int. J. Chron. Obstruct. Pulmon. Dis. *8*, 151–157. https://doi.org/10.2147/copd.S39403.

57. Payne, G.A., Li, J., Xu, X., Jackson, P., Qin, H., Pollock, D.M., Wells, J.M., Oparil, S., Leesar, M., Patel, R.P., et al. (2017). The Matrikine Acetylated Proline-Glycine-Proline Couples Vascular Inflammation and Acute Cardiac Rejection. Sci. Rep. *7*, 7563. https://doi.org/10.1038/s41598-017-07610-0.

STAR★METHODS

KEY RESOURCES TABLE

REAGENT or RESOURCE	SOURCE	IDENTIFIER
Antibodies		
Mouse anti-VE-cadherin (CD144)	eBioscience	Cat# 16–1441; RRID: AB_2865876
Rat IgG1 kappa isotype control	eBioscience	Cat# 16–4301; RRID: AB_2865968
Mouse anti-Ly6G (clone 1A8)	BioXCell	Cat# BE0075-1; RRID: AB_1107721
Rat IgG2a isotype control (clone 2A3)	BioXCell	Cat# BE0089; RRID: AB_1107769
Rat anti-Mouse CD16/CD32 (Mouse Fc Block™)	BD Biosciences	Cat# 553142; RRID: AB_394657
Rat anti-Mouse Ly6G FITC (clone 1A8)	BD Biosciences	Cat# 561105; RRID: AB_10562567
Anti-Mouse/human CD11b PerCP (clone M1/70)	BioLegend	Cat# 101230; RRID: AB_2129374
Hamster anti-Mouse CD11c APC (clone HL3)	BD Biosciences	Cat# 550261; RRID: AB_398460
Anti-Mouse F4/80 PE (clone BM8)	eBioscience	Cat# 12-4801-82; RRID: AB_465923
Goat anti-LTA4H (clone C-21)	Santa Cruz Biotechnology	Cat# sc-23070; RRID: AB_2138750
Donkey anti-Goat IgG HRP	Santa Cruz Biotechnology	Cat# sc-2020; RRID: AB_631728
Human/Mouse Leukotriene A4 Hydrolase antibody	Bio-Techne	Cat# AF4008; RRID: AB_2044691
Rabbit anti-Sheep IgG (H + L) secondary HRP	Bio-Techne	Cat# NB7195; RRID: AB_524685
Biological samples		
Human peripheral blood	Imperial College London, National Heart and Lung Institute	N/A
Chemicals, peptides, and recombinant proteins		
LIVE/DEAD Fixable Near-IR-Dead Cell stain	Thermo Fisher Scientific	L34976
Synthetic triacylated lipopeptide (Pam3CSK4)	InvivoGen	tlrl-kit1mw
Heat Killed *Listeria monocytogenes* (HKLM)	InvivoGen	tlrl-kit1mw
Polyinosine-polycytidylic acid (Poly(I:C))	InvivoGen	tlrl-kit1mw
Lipopolysaccharide from *Escherichia coli* K12 (LPS-EK)	InvivoGen	tlrl-kit1mw
LPS-EK Ultrapure	InvivoGen	tlrl-peklps
Flagellin from *Salmonella typhimurium*	InvivoGen	tlrl-kit1mw
Synthetic diacylated lipoprotein (FSL-1)	InvivoGen	tlrl-kit1mw
Single-stranded RNA (ssRNA)	InvivoGen	tlrl-kit1mw
CpG oligonucleotide (ODN1826)	InvivoGen	tlrl-kit1mw
Mouse recombinant IL-1β	R&D Systems	401-ML/CF
Mouse recombinant IL-1β	PeproTech	211-11B
Mouse recombinant MIP-2	PeproTech	250–15
Histamine	Sigma-Aldrich	H7125
Brefeldin A	Enzo Life Sciences	BML-G405
Human recombinant TNF	PeproTech	300-01A
Human recombinant IL-6	PeproTech	200–06
Human recombinant IL-1β	PeproTech	200-01B
Calcium ionophore A23187	Sigma-Aldrich	A23187
Pro-Gly-Pro (PGP)	Bachem	H-7284
Ninhydrin	Sigma-Aldrich	151173
Recombinant Leukotriene A4 Hydrolase Protein	Sino Biological	50268-M08B
Critical commercial assays		
Lactate Dehydrogenase Activity Assay Kit	Sigma-Aldrich	TOX7
Mouse LTA4H ELISA kit	Cloud-Clone Corp	E93236MU
Mouse Albumin ELISA kit	Bethyl Laboratories	E99-134

(*Continued on next page*)

Continued

REAGENT or RESOURCE	SOURCE	IDENTIFIER
LTB4 assay kit	R&D Systems	KGE006B
MTT assay kit	Sigma-Aldrich	TOX-1
Mouse ALT ELISA kit	Abcam	ab282882
Deposited data		
Raw Western blot data	This paper	https://doi.org/10.17632/yyyz76tsp5.1
Experimental models: Cell lines		
Human hepatocellular carcinoma (HepG2)	ATCC	Cat# HB-8065; RRID: CVCL_0027
Experimental models: Organisms/strains		
Mouse strain: wild-type BALB/c	Envigo	162
Mouse strain: wild-type BALB/c	Charles River UK	028
Mouse strain: *Lta4h*$^{+/+}$ (littermate controls 129/S)	Central Biological Services, Imperial College London	N/A
Mouse strain: *Lta4h*$^{+/-}$ (heterozygote)	Central Biological Services, Imperial College London	N/A
Mouse strain: *Lta4h*$^{-/-}$ (homozygote)	Central Biological Services, Imperial College London	N/A
Oligonucleotides		
LTA4H MUTF primer: CTTGGGTGGAGAGGCTATTC	Invitrogen	N/A
LTA4H MUTR primer: AGGTGAGATGACAGGAGATC	Invitrogen	N/A
LTA4H WTF primer: CGAATCCATGCTTAAAATTGC	Invitrogen	N/A
LTA4H WTR primer: GCGTTACGAACGTGAGACAA	Invitrogen	N/A
Other		
Infusion/Withdrawal Syringe Pump	Harvard Apparatus Limited	50–4928

RESOURCE AVAILABILITY

Lead contact

Further information and requests for resources and reagents should be directed to and will be fulfilled by the lead contact, Professor Robert Snelgrove (robert.snelgrove@imperial.ac.uk).

Materials availability

This study did not generate new unique reagents.

Data and code availability

- Original western blot images have been deposited at Mendeley and are publicly available as of the date of publication. The DOI is listed in the key resources table. All additional data reported in this paper will be shared by the lead contact upon request.
- This paper does not report original code.
- Any information required to analyze the data reported in this paper is available from the lead author upon request.

EXPERIMENTAL MODEL AND STUDY PARTICIPANT DETAILS

Mice

All mouse experiments were performed in accordance with the recommendations in the Guide for the Use of Laboratory Animals of Imperial College London, with the ARRIVE (Animal Research: Reporting of *In Vivo* Experiments) guidelines. All animal procedures and care conformed strictly to the UK Home Office Guidelines under the Animals (Scientific Procedures) Act 1986, and the protocols were approved by the Home Office of Great Britain. All mice were kept in specified pathogen-free conditions and provided autoclaved food, water and bedding, and were randomly assigned to experimental groups. Eight-to 12-week-old female Balb/c mice were purchased from Envigo or Charles River UK. All *Lta4h*$^{-/-}$ mice and littermate controls, on a 129/S background, were provided by Y.M. Shim and subsequently bred in house. *Lta4h*$^{-/-}$ and littermate controls were genotyped by PCR on genomic DNA extracted using the Extract-N-Amp Tissue PCR Kit (Sigma-Aldrich). Wild-type expression of LTA_4H was detected by primers oIMR1720 (50-CGAATCCA TGCT TAAAATTGC-30) and oIMR1721 (50-GCGTTACGAACGTGAGACAA-30) to yield a product size of 128 bp, whilst mutant LTA_4H was detected by primers oIMR6916 (50-CTTGGGTGGAGAGGCTATTC-30) and oIMR6917 (50-AGGTGA GATGACAGGAGATC-30)

to yield a product size of 280 bp. Amplification was achieved by PCR (94°C for 3min > 35 × 2.5 min cycles (30 s at 94°C > 60 s at 60°C > 60 s at 72°C) > 72°C for 2 min). Amplification fragments were visualized on 2% agarose gels.

METHOD DETAILS

Mouse challenge models

Toll-like receptor (TLR) agonist administration

Female Balb/c mice were intranasally (i.n.) administered a single dose of agonists to specific TLRs (InvivoGen mouse TLR Agonist Kit) in 50 μL sterile PBS. Specifically, mice were administered Pam3CSK4 (TLR1/2 agonist; 1 μg), HKLM (TLR2 agonist; 1 x 10^8 bacteria), Poly(I:C) (TLR3 agonist; 50 μg), LPS (TLR4 agonist; 10 μg), Flagellin (TLR5 agonist; 1 μg), FSL-1 (TLR6/2 agonist; 1 μg), ssRNA (TLR7 agonist; 2.5 μg) or ODN1826 (TLR9 agonist; 10 μg). Control mice were administered 50 μL sterile PBS intranasally. All mice were culled 24 h post administration of TLR agonist/vehicle control. In some experiments, mice were intranasally (i.n.) administered a single dose of LPS (10 μg LPS-EK Ultrapure; Invivogen) in 50 μL sterile PBS and culled 6, 12 or 24 h later.

In vivo *neutrophil depletion*

To deplete neutrophils, female Balb/c mice received intraperitoneal (i.p.) administration of 100 μg of anti-Ly6G (clone 1A8; BioXCell) in 200 μL of PBS. Control mice received 200 μg of isotype control antibody (clone 2A3; BioXCell) in 200 μL of PBS. Mice were administered the respective antibodies on alternate days throughout the experiment as described in respective figure legends.

Administration of MIP-2

Female Balb/c mice were intranasally (i.n.) administered 1 μg MIP-2 in 50 μL sterile PBS. Control mice were administered 50 μL sterile PBS i.n. All mice were culled after 6 h.

Histamine administration

Female Balb/c mice were intravenously (i.v.) administered 5 mg histamine (Sigma-Aldrich) in 200 μL sterile PBS. Control mice were administered 200 μL sterile PBS i.v. All mice were culled after 30 min.

Administration of anti-VE-cadherin antibody

Female Balb/c mice were intravenously (i.v.) administered 200 μg of anti-VE-cadherin (CD144) antibody (BV13; eBioscience) in 200 μL sterile PBS. Control mice were administered 200 μg of rat IgG1 isotype control antibody in 200 μL sterile PBS i.v. All mice were culled after 7 h.

Acute phase response stimulants

Female Balb/c mice were intraperitoneally (i.p.) administered 80 ng mouse recombinant IL-1β (R&D Systems) in 200 μL sterile PBS. Control mice received 200 μL sterile PBS i.p. All mice were culled after 6 h.

Mouse tissue isolation and processing

Mice were euthanized by intraperitoneal injection of sodium pentobarbital (Pentoject; Animalcare United Kingdom) followed by exsanguination via cardiac puncture and serum subsequently isolated by centrifugation for 8 min at 5,000 x g and then stored at −80°C for downstream analysis. To obtain blood plasma, blood was immediately admixed with 100 μL citrate dextran solution and centrifuged at 800 x g for 5 min. Plasma was subsequently decanted, and the remaining cell pellet was washed 2 × 5 min with 0.5 mL PBS before lysis in 200 μL dH_2O. Plasma and cell extract was subsequently stored at −80°C for downstream analysis.

Bronchoalveolar lavage (BAL) was performed by inflating the lungs 4 times each with 1.2 mL of PBS via a tracheal cannula. The BAL fluid was then centrifuged at 800 x g for 5 min after which the BAL supernatant was collected and frozen at −80°C until required. The remaining cell pellet was re-suspended in 0.5 mL complete media (R10F; RPMI (Thermo Fisher) supplemented with 10% heat inactivated fetal bovine serum).

For downstream analysis of LTA_4H concentrations and PGP-degrading activity, liver tissue was homogenized at a concentration of 200 mg/mL in PBS. Liver homogenates were centrifuged at 10,000 x g for 10 min, and supernatants stored at −80°C for downstream analysis. For downstream Western blot analysis of LTA_4H, liver was homogenized in 3 mL RIPA buffer (containing PMSF, protease inhibitor and sodium orthovanadate; Santa Cruz Biotechnology)/gram of tissue. Tissue homogenate was stored on ice for 30 min, prior to centrifugation at 10,000 x g for 10 min, and ensuing storage of supernatants at −80°C for downstream analysis.

Primary mouse hepatocyte isolation

Mice were euthanized by intraperitoneal (i.p.) injection of sodium pentobarbital (Pentoject) followed by confirmation of death via exsanguination of the femoral artery. The superior vena cava and portal vein were exposed and a 25-guage needle connected to an infusion/withdrawal syringe pump (Harvard Apparatus Scientific) via 2 mm clear tubing was inserted into the superior vena cava above the kidneys. Pre-warmed (42°C) perfusion buffer (HBSS (no Ca^{2+}/Mg^{2+}/phenol red; Thermo Fisher Scientific) + 0.5 mM EDTA (Invitrogen) + 25 mM HEPES (Sigma Aldrich)) was infused through the liver at a rate of 1 mL/min and the portal vein cut upon swelling, with a total perfusion duration of 10 min. Following perfusion, pre-warmed (42°C) digestion buffer (DMEM low glucose (Thermo Fisher Scientific) + 25 mM HEPES +25 μg/mL Liberase (Roche)) was infused through the liver at a rate of 1 mL/min for 10 min. The liver was removed, dissociated, filtered through a 70μm cell strainer (Corning) into a 50 mL centrifuge tube and centrifuged at 50 x g for 2 min at 4°C and low acceleration/deceleration. The supernatant was aspirated, pellet resuspended in 10 mL DMEM (low glucose) + 1% penicillin-streptomycin and mixed with a 90% Percoll (Sigma Aldrich) solution, followed by

centrifugation at 200 x g for 10 min at 4°C. The supernatant was aspirated, pellet resuspended in 20 mL DMEM (low glucose) + 1% penicillin-streptomycin and centrifuged at 50 x g for 2 min at 4°C and low acceleration/deceleration. The supernatant was aspirated, and the pellet resuspended in 20 mL DMEM (low glucose) + 1% penicillin-streptomycin for counting via trypan blue. Immediately following isolation, 5 x 10^5 hepatocytes were resuspended in 1 mL RIPA buffer (containing PMSF, protease inhibitor and sodium orthovanadate; Santa Cruz Biotechnology) and stored at −80°C for downstream analysis.

Primary mouse hepatocyte culture and stimulation

Primary mouse hepatocytes were seeded at 5 x 10^5 cells/well in DMEM (low glucose) + 5% fetal calf serum (FCS) + 1% penicillin-streptomycin in a 24-well plate (Nunc) coated with 0.01% rat-tail collagen (Sigma-Aldrich) at 37°C and 5% CO_2 for 3 h to allow adhesion. After 3 h, all media was replaced with 1 mL maintenance media (William's E media-GlutaMAX (Thermo Fisher Scientific) + 1% penicillin-streptomycin). In specific experiments (as defined in respective figure legends), primary mouse hepatocytes were cultured in maintenance media containing 10 μg/mL Brefeldin A (Enzo Life Sciences) or recombinant murine IL-1β (1 ng/mL; PeproTech). Following stimulation, cells were centrifuged at 800 x g for 10 min, and supernatants stored at −80°C while cell monolayers were resuspended in 200 μL RIPA buffer (containing PMSF, protease inhibitor and sodium orthovanadate) on ice for 15 min and stored at −80°C for downstream analysis.

Human samples

Whole blood was obtained from healthy volunteers by phlebotomy into heparinized vacuum phlebotomy vials. Red blood cells (RBCs) were allowed to sediment for 20 min at 20°C after 1:1 mixture with 5% dextran. Supernatant was eluted and centrifuged for 7 min at 1,000 x g at 20°C. Residual RBCs were lysed by resuspending the pellet in ice-cold 0.2% saline for 30 s then rapidly bringing solution to isotonicity with 1.6% saline. The cell pellet was resuspended in filter-sterilized 0.9% saline solution equal to starting volume of whole blood and 10 mL of Ficoll gradient solution (GE Healthcare BioSciences) was layered at the bottom of a 50 mL centrifuge tube. This was then centrifuged for 40 min at 1000 x g at 4°C to separate Polymorphonuclear neutrophils (PMNs) and peripheral blood mononuclear cells (PBMCs). Approval was granted by the Brompton, Harefield and National Heart and Lung Institute ethics committee and informed written consent was provided by all volunteers prior to sample collection.

HepG2 culture and stimulation

Human hepatocellular carcinoma cell line, HepG2s (ATCC), were cultured and expanded in minimum essential media (MEM; ATCC) containing 10% FCS at 37°C and 5% CO_2. For experiments, HepG2 cells were cultured at 5 x 10^5 cells/well of a 24 well plate in serum free media at 37°C and 5% CO_2 for variable periods of time (as defined in respective figure legends). In some experiments, HepG2 cells were cultured in media containing 10 μg/mL Brefeldin A. In other experiments, HepG2 cells were cultured in media containing recombinant human TNF (10 ng/mL; PeproTech), IL-6 (10 ng/mL; PeproTech), IL-1β (1 ng/mL; PeproTech) or a combination of IL-6 and IL-1β (10 and 1 ng/mL, respectively). Following stimulation, cells were centrifuged at 800 x g for 10 min, and supernatants stored at −80°C for downstream analysis.

PGP degradation experiments

BAL fluid, serum, liver homogenate, primary mouse hepatocyte culture supernatant or HepG2 supernatant (diluted in PBS as defined in respective figure legends) was incubated with 100 μg/mL PGP (Bachem) at 37°C and 5% CO_2 for variable periods of time (as defined in respective figure legends). Concentrations of remaining PGP were quantified by ESI–LC/MS/MS (as described below) by comparison with PGP standards. The percentage of peptide degraded was determined relative to control samples of 100 μg/mL PGP alone. PGP degradation was also assessed by liberation of the N-terminal proline of PGP and its ensuing reaction with Ninhydrin (as described below).

ESI–LC/MS/MS for PGP detection

For peptide quantification from degradation experiments, PGP was measured using a Thermo Accela Pump and Autosampler coupled to a ThermoTSQ Quantum Access. HPLC was done using a 2.0x150-mm Jupiter 4u Proteo column (Phenomenex) with A: 0.1% HCOOH and B: MeCN+0.1% HCOOH: 0–0.5 min 5% buffer B/95% buffer A, then increased over 0.5–2.5 min to 100% buffer B/0% buffer A. Background was removed by flushing with 100% isopropanol/0.1% formic acid. Positive electrospray mass transitions were at 270-70, 270-116, and 270-173 for PGP. Peak area was measured, and peptide concentrations were calculated relative to heavy labeled PGP internal standard (Bachem) using a relative standard curve method as previously described.[14]

Measurement of free proline

Aliquots from PGP degradation experiments were diluted 1 in 10 in PBS to a final volume of 250 μL. Glacial acetic acid (250 μL) was then added, followed by 250 μL of Ninhydrin (Sigma-Aldrich) solution (25 mg/mL in acetic acid/6 M phosphoric acid; heated at 70°C to dissolve). The reaction mixture was heated at 100°C for 60 min, allowed to cool to room temperature and the proline containing fraction extracted with 500 μL of toluene and optical density measured at 520 nm.

LTA_4H epoxide hydrolase activity and LTB_4 generation

A total of 2 x 10^5 HepG2 cells or human peripheral blood neutrophils in 200 μL RPMI were treated with calcium ionophore A23187 (Sigma-Aldrich) at a final concentration of 2 μg/mL 1% DMSO was used as a control. Cells were incubated for 20 min at 37°C, and supernatants removed and stored at −80°C for subsequent LTB_4 analysis. The concentration of LTB_4 in cell supernatants was assayed using an ELISA, according to manufacturer's directions (R&D systems).

Quantification of soluble mediators

The concentration of LTA_4H in mouse BAL fluid, serum and liver homogenate were assessed using an ELISA, according to the manufacturer's instruction (USCN Life Science).

Lactate dehydrogenase (LDH) activity in mouse BAL fluid was assessed using the Lactate Dehydrogenase Activity Assay Kit (Sigma-Aldrich). Equal volumes of LDH substrate, LDH assay dye and LDH assay cofactor preparation were combined and 100 μL was added to 50 μL of sample. The samples were incubated at room temperature in the dark for 30 min. The reaction was stopped using 30 μL 1N HCl and absorbance determined using a spectrophotometer (490 nm; Tecan microplate reader).

Flow cytometry

Cells were stained with the LIVE/DEAD Fixable Near-IR-Dead Cell staining kit (Molecular Probes, Invitrogen) for 10 min in PBS before being blocked with anti-CD16/CD32 Fc receptor block (BD Biosciences) for 20 min. Cells were then washed in PBS and stained for surface markers for 30 min at 4°C in PBS containing 0.1% (w/v) sodium azide and 1% (w/v) BSA and were fixed with 2% (v/v) paraformaldehyde. All samples were acquired immediately on a BD LSR Fortessa cell analyzer (BD Biosystems) and analyzed using BD FACSDIVA (BD Biosystems). To identify neutrophils, cells were stained with anti-Ly6G-FITC (1A8; BD Biosciences; 1/100 dilution), anti-CD11b-PerCP (M1/70; eBioscience; 1/400 dilution), anti-CD11c-APC (HL3; BD Biosciences; 1/200 dilution) and anti-F480-PE (BMB; eBioscience; 1/50 dilution), with neutrophils defined as Ly-$6G^{high}$ $CD11b^{high}$ $CD11c^{low}$ $F4/80^{low}$.

Western blot

Cell or tissue lysates (at concentrations defined in respective figure legends) were admixed with 10 x reducing agent (Thermo Fisher) and 4 x loading buffer (Thermo Fisher), and then heated at 100°C for 5 min. Samples were cooled on ice and loaded into NuPAGE 4–12% Bis-Tris Protein Gels (Thermo Fisher) prior to electrophoresis in NuPAGE MES SDS Running Buffer (Thermo Fisher) at 125 V for 90 min. Separated proteins were subsequently transferred on to nitrocellulose membranes in NuPAGE Transfer Buffer (Thermo Fisher) at 35 V for 90 min. Membranes were blocked in PBS containing 5% milk and 0.1% Tween 20 for 2 h at room temperature with gentle agitation. Membranes were then incubated with either goat anti-LTA_4H antibody (C-21; 1/500; Santa Cruz) or Human/Mouse anti-LTA_4H antibody (PMHs only; Bio-Techne) in PBS containing 5% milk and 0.1% Tween 20 overnight at 4°C with gentle agitation. Membranes were subsequently washed 3 × 15 min in PBS/0.1% Tween 20 at room temperature, prior to incubation with either donkey anti-goat-HRP (1/5000; Santa Cruz) or rabbit anti-sheep IgG HRP (PMHs only; Bio-Techne) in PBS containing 5% milk and 0.1% Tween 20 for 2 h at room temperature with gentle agitation. Membranes were again washed, and reactivity was detected utilizing ECL2 Western Blotting Substrate kit (ThermoFisher Scientific) according to manufacturer's instructions.

Immunohistochemistry of liver tissue

Liver tissue was fixed in 10% neutral buffered formalin for 24 h before paraffin wax embedding. Paraffin embedded sections (4 μm thick) were subsequently dewaxed in Histoclear (2 × 15 min; National Diagnostics) followed by two washes in absolute alcohol. Tissue endogenous peroxidases were blocked by incubation in methanol containing 1% H_2O_2 for 10 min. Antigen retrieval was performed in 10 mM trisodium citrate solution, pH 6, heated in a microwave for 10 min. Tissue sections were subsequently transferred to PBS prior to avidin-biotin blocking, according to manufacturer's instructions. Tissue sections were blocked for 1 h at room temperature in PBS containing % goat serum and 0.1% BSA. Sections were subsequently incubated with goat anti-LTA_4H antibody (C-21; 2 μg/mL; SantaCruz) diluted in PBS containing 5% goat serum and 0.1% BSA overnight at 4°C in a humidified chamber. Sections were washed in PBS containing 0.1% Triton X- and 0.1% BSA (3 × 5 min), and then incubated in donkey anti-goat-HRP (4 μg/mL; SantaCruz) diluted in PBS containing 5% donkey serum and 0.1% BSA for 2 h at room temperature. Cells were again washed in PBS containing 0.1% Triton X- and 0.1% BSA (3 × 5 min) and incubated with DAB substrate for 10 min and ensuing counterstain with hematoxylin.

QUANTIFICATION AND STATISTICAL ANALYSIS

Statistical significance was calculated with a nonparametric Mann-Whitney test (two-sided) and Prism software (GraphPad Software Inc.). Results are depicted as means ± SEM unless stated otherwise. Statistical significance for correlations was calculated using a Spearman rank test with *p* values and r values noted on the respective graphs. $*p < 0.05$, $**p < 0.01$, $***p < 0.001$, and $****p < 0.0001$ were considered significant and are referred to as such in the text. Details of specific statistical tests used for individual analysis and number of replicates are detailed in respective Figure Legends.